Accurate Theoretical Study of the Excited States of Boron and Aluminum Carbides, BC, AlC. 2

Demeter Tzeli and Aristides Mavridis*

Laboratory of Physical Chemistry, Department of Chemistry, National and Kapodistrian University of Athens, P.O. Box 64 004, 157 10 Zografou, Athens, Greece

Received: February 7, 2001; In Final Form: May 14, 2001

Continuing our study on the electronic structure of the carbides BC and AlC (Tzeli, D.; Mavridis, A. *J. Phys. Chem. A* **2001**, *105*, 1175), we have investigated the electronic structure of 29 and 30 excited states of the BC and AlC molecules, respectively, by ab initio quantum mechanical multireference methods and quantitative basis sets. For both diatomic species we report complete potential energy curves, total energies, interatomic distances, dissociation energies, dipole moments, Mulliken charges, energy gaps, and usual spectroscopic constants. Our results are, in general, in good to very good agreement with the existing experimental values.

1. Introduction

Recently, we investigated the ground-state electronic structures of the BC and AlC molecules using multireference variational methods and large correlation consistent basis set.[1] It was found that the ground state of both molecular systems is of $^4\Sigma^-$ symmetry, with calculated (experimental) dissociation energies (D_e) and equilibrium bond distances (r_e) of (D_e, kcal/mol; r_e, Å) = 102.3 (106 ± 7[2]), 1.4911 (1.49116 ± 0.00034[3]), and 80 (64.92[4]), 1.963 (1.95503[5]) for BC and AlC, respectively. Notice the ∼15 kcal/mol difference between theory and experiment in the D_e value of the AlC system.

Presently, we focus on the investigation of the BC and AlC excited states, following a similar calculational approach as in ref 1. The states examined ensue from the interaction of the atomic fragments $|^{2S_1+1}L_1\rangle \times |^{2S_2+1}L_2\rangle$ = [B (^{2}P, ^{4}P), Al (^{2}P, ^{2}S, ^{4}P)] × C (^{3}P, ^{1}D, ^{1}S, ^{5}S), a total of 64 and 74 states of $^{2S+1}|\Lambda|$ type, where Λ is the projection of the total orbital angular momentum along the internuclear axis. In particular, the following states have been examined for both molecules, $^2\Sigma^+$(2), $^2\Sigma^-$(2), $^4\Sigma^+$(2), $^4\Sigma^-$(3), $^6\Sigma^+$(2), $^6\Sigma^-$(2), $^2\Pi$(4), $^4\Pi$(4), $^6\Pi$(3), $^2\Delta$(2), $^4\Delta$(2), $^6\Delta$(1), $^4\Phi$(1) plus one $^2\Phi$ state for the AlC molecule, a total of 30 (BC) and 31 (AlC) states including the ground $X^4\Sigma^-$ states. We report full potential energy curves (PEC), dissociation energies (D_e), bond lengths (r_e), dipole moments (μ), Mulliken charges (q), energy gaps (T_e), and certain spectroscopic constants (ω_e, $\omega_e x_e$, α_e, $\bar{D}_e$).

As early as 1970, Kouba and Öhrn[6] had examined 54 (19 bound) states of the BC molecule using a minimal Slater basis set and a natural orbital configuration interaction (CI) approach, identifying correctly the ground and the qualitative ordering of few excited states. We are aware of two more theoretical works on the excited states of the BC system. In 1986 Zaitsevskii et al.,[7] examined in addition to the $X^4\Sigma^-$ state, the $^2\Pi$, $^2\Delta$, and $^2\Sigma^-$ excited states using an effective core potential approximation and a DZ+P basis. In 1987 Hirsch and Buenker[8] applying the MRD−CI method coupled with a $[6s4p1d]_{B,C}$ basis, calculated 19 excited states, reporting PECs up to 4.2 bohr for 13 states and spectroscopic constants (r_e, ω_e, and $\omega_e x_e$) for 11 states.

Experimental findings on the BC molecule are rather limited. Fernando et al., (Fourier transform emission spectroscopy),[3] Smith et al., (Fourier transform spectroscopy in solid Ne matrices),[9] and Wyss et al. (electronic absorption spectra in neon matrices)[10] report on the $A^4\Pi$,[9] $B^4\Sigma^-$,[3,9,10] $a^2\Pi$,[9] $d^2\Sigma^+$,[9] and $C^4\Pi$[10] states (vide infra).

Concerning the theoretical literature on the excited states of AlC, there is the work of Zaitsevskii et al.,[7] reporting on the $^2\Pi$, $^2\Delta$, and $^2\Sigma^-$ (excited) states, and the very recent work of Bartlett and co-workers[11] who examined, in addition to the $X^4\Sigma^-$, the $a^2\Pi$, and $A^4\Pi$ states of AlC via the CCSD(T)/[7s7p5d4f/7s7p4d3f] method focusing on absolute energies, r_e, and ω_e values, and finally the more extensive work of Bauschlicher and co-workers.[12] These workers employing the complete active space self-consistent field + singles + doubles excitations (CASSCF+1+2 = MRCI) method in conjunction with a [5s4p2d1f/4s3p2d1f] basis, calculated 18 excited states. For 11 (excited) states they report r_e, ω_e, and T_e values and PECs up to 4.4 bohr, while the rest of the seven states are treated at the CASSCF level; no absolute energies are given for any state.[12]

On the experimental side we are aware of two reports on the AlC molecule: Thoma et al.,[4] using Fourier transform fluorescence spectroscopy in solid argon, and Brazier,[5] using emission spectroscopy, examined the AlC $B^4\Sigma^-$ state. They report ω_e, $\omega_e x_e$, and T_e,[4,5] D_e[4], and r_e[5] values (vide infra).

In section 2 we discuss some computational details, in section 3 we give B, C, and Al atomic results followed by an analysis of all molecular states. Finally, section 4 contains a synopsis of our findings and some remarks.

2. Computational Methods

For all atoms the correlation consistent (cc) basis sets of Dunning and co-workers were employed.[13] In particular, for the BC molecule we have used the quintuple quality basis but with the *h* angular momentum functions removed, i.e., cc-pV5Z-h = $(14s8p4d3f2g)_{B,C}$, generally contracted to $[6s5p4d3f2g]_{B,C}$, numbering 160 spherical Gaussian functions. For the AlC system the augmented quadruple quality basis was used, aug-cc-pVQZ = $(17s12p4d3f2g/_{Al}\ 13s7p4d3f2g/_C)$,

10.1021/jp010459v CCC: $20.00
Published on Web 07/20/2001

TABLE 1: Calculated and Experimental Atomic Energy Separations (eV) of B ($^4P \leftarrow {}^2P$), C ($^1D \leftarrow {}^3P$, $^1S \leftarrow {}^3P$, $^5S \leftarrow {}^3P$), and Al ($^2S \leftarrow {}^2P$, $^4P \leftarrow {}^2P$) Atoms

	B		C		Al	
method	$^4P \leftarrow {}^2P$	$^1D \leftarrow {}^3P$	$^1S \leftarrow {}^3P$	$^5S \leftarrow {}^3P$	$^2S \leftarrow {}^2P$	$^4P \leftarrow {}^2P$
CAS[a]	2.984	1.504	2.613	2.906	2.499	2.832
MRCI[b]	3.595	1.270	2.673	4.121	3.158	3.445
MRCI+Q[c]	3.62	1.26	2.68	4.19	3.20	3.49
exptl[d]	3.571	1.260	2.680	4.179	3.133	3.598

[a] Spherically averaged CASSCF. [b] Internally contracted MRCI. [c] MRCI + Davidson correction. [d] Reference 17.

similarly contracted to [7s6p4d3f2g/$_{Al}$ 6s5p4d3f2g/$_{C}$] containing 164 spherical Gaussians.

Our calculational approach is that of complete active space SCF (CASSCF) + single + double excitations out of the CASSCF (reference) space (MRCI), in conjuction with the internal contraction (ic) technique.[14] Our largest MRCI expansion for the BC/AlC molecules contains 7184 828/13 516 872 configuration functions (CFs), internally contracted to 843 000/1153 000 CFs. Estimated energy losses due to the ic method are rather small,[15] and do not seem to influence the quality of our results.[1,15] In addition, and mainly for technical reasons, we were forced to resort to state average (SA)[16] CASSCF calculations almost for all, but the ground states.

Our reference space is comprised of eight and nine orbitals for the BC and AlC molecules respectively, viz., $(2s + 2p_x + 2p_y + 2p_z) \times 2$ (BC), and $(3s + 3p_x + 3p_y + 3p_z + 4s + 2s + 2p_x + 2p_y + 2p_z)$ (AlC), correlating seven valence electrons. Core B ($1s^2$), C ($1s^2$), and Al ($1s^22s^22p^6$) electrons were always kept doubly occupied at the CI level. The extra 4s orbital in the AlC reference space was deemed as necessary due to the Rydberg character of the first excited state (^2S) of the Al atom. It is of interest to note that of all elements reported in the Moore Tables,[17] only the atoms of the 13th (IIIA) column, but boron, have a first excited state of Rydberg (^2S) character. Finally, all our CASSCF states display symmetry and equivalence restrictions, and at the MRCI level size nonextensivity errors range from 1 to 3 mhartree, as is revealed by taking the energy difference between the supermolecule and the energy sum of the two atoms at the same level of theory.

Through all this work computations were performed with the MOLPRO96[18] suite of codes.

3. Results and Discussion

3.1. Atomic States. Table 1 lists atomic energy splittings of B ($^4P \leftarrow {}^2P$), C (^5S, ^1S, $^1D \leftarrow {}^3P$), and Al (^4P, $^2S \leftarrow {}^2P$) at the CASSCF (spherically averaged), MRCI, and MRCI + multireference Davidson correction (+Q)[19] level of theory, along with corresponding experimental results.[17] The overall agreement between theory and experiment at the CASSCF level is tolerable, but good at the MRCI, the largest discrepancy being 0.15 eV (Al, $^4P \leftarrow {}^2P$); interestingly, all splittings are consistently improved by including the +Q Davidson empirical correction.

3.2. Molecular States. In what follows we analyze first all doublets, then the quartets, and finally the sextets. Figure 1 shows a relative energy diagram of all bound states, with similar BC and AlC electronic states connected by lines. Each molecular state has been tagged with a serial number in front of the term symbol indicating its absolute energy order with respect to the ground (X) state. A second number into parenthesis refers to the ordering of states according to energy within the same space−spin symmetry manifold. Subscripts G and L mean "global" and "local" minima in the potential energy curves,

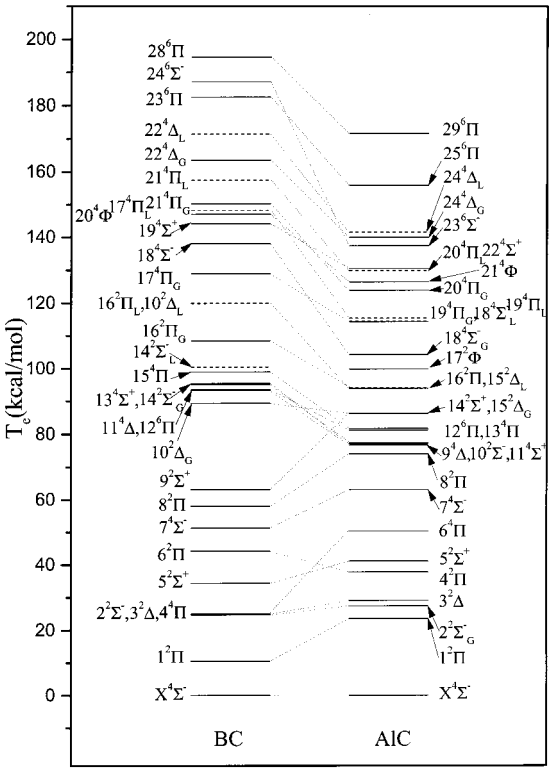

Figure 1. Relative energy levels of the isovalent species BC and AlC at the MRCI level. Thin lines connect similarly bound states of the two molecules. G and L refer to global and local minima, respectively.

respectively. Tables 2 and 3 include total energies (E), dissociation energies (D_e), bond distances (r_e), spectroscopic constants (ω_e, $\omega_e x_e$, α_e, $\bar{D}_e$), dipole moments (μ), Mulliken charges on carbon (q_C), and energy splittings (T_e) of BC and AlC, respectively at the CASSCF, MRCI and MRCI+Q level of theory. Existing experimental results are also included. Tables 4, and 5 give asymptotic fragments, dominant equilibrium CASSCF CFs, C_{2v} symmetries, and equilibrium Mulliken atomic populations. Finally, Figures 2 through 13 show MRCI potential energy curves (PEC) of all states studied.

3.2.a. Symmetries $^2\Sigma^+$, $^2\Sigma^-$, $^2\Pi$, $^2\Delta$, *and* $^2\Phi$. $5^2\Sigma^+(1)$, $9^2\Sigma^+(2)$/$5^2\Sigma^+(1)$, $14^2\Sigma^+(2)$. The first entry will always refer to BC and the second to the AlC molecular states. For both systems, the $5^2\Sigma^+$ states are similar in every respect. Tables 4 and 5 suggest that the bonding is comprised of one π and $^1/_2$ σ bonds, indicated by the following valence-bond-Lewis (vbL) icon (Z = B or Al),

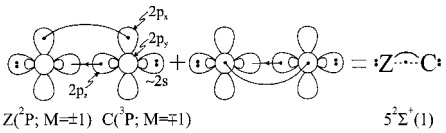

Along the π frame 0.2/0.5 e^- are transferred from B/Al to the C atom, with less than 0.1 e^- from C to Z through the σ frame, resulting in a net transfer of 0.15 and 0.4 e^- to the C atom in BC and AlC, respectively. At the MRCI level we obtain D_e = 66.6 (BC), and 36.9 (AlC) kcal/mol with respect to the ground-state atoms.

Experimentally, for the $d^2\Sigma^+$ state of the BC, ω_e = 1031.1 cm^{-1} and T_e ($d^2\Sigma^+ \leftarrow a^2\Pi$) = 32.052 kcal/mol.[9] These values should be contrasted with our MRCI values (Table 2), ω_e ($5^2\Sigma^+$) = 1123 cm^{-1}, and T_e ($5^2\Sigma^+ \leftarrow 1^2\Pi$) = 23.8 kcal/mol. Being confident about our findings, we express some reservations about the experimental values.

TABLE 2: Absolute Energies E (hartree), Dissociation Energies D_e (kcal/mol), Bond Distances r_e (Å), Harmonic Frequencies ω_e (cm^{-1}), First Anharmonic Corrections $\omega_e x_e$ (cm^{-1}), Rotational Vibrational Couplings α_e (cm^{-1}), Centrifugal Distortions $\bar{D}_e$ (cm^{-1}), Dipole Moments μ (D), Mulliken Charges on the C Atom q_c, and Energy Gaps T_e (kcal/mol) for 30 States of the $^{11}B^{12}C$ Molecule, at the CASSCF, MRCI,[a] and MRCI+Q[b]/cc-pV5Z-h Levels of Theory. "G" and "L" Subscripts Refer to Local and Global Minima

State	Method	−E	D_e	r_e	ω_e	$\omega_e x_e$	α_e (10^{-2})	$\bar{D}_e$ (10^{-6})	μ	q_c	T_e
$X^4\Sigma^-$	CASSCF	62.41873	92.2	1.509	1134.8	10.1	1.06	6.66	0.779	−0.17	0.0
	MRCI	62.54526	100.7	1.498	1161.1	11.0	1.67	6.65	0.942	−0.16	0.0
	MRCI+Q	62.5523	100.9	1.499							0.0
	MRCI[c]	62.646425	102.06	1.4919	1173.5	10.12	1.64	6.67	0.939	−0.19	
	CBS[d]	62.6489 ± 4	102.3 ± 0.1	1.4911 ± 3	1176 ± 1				0.945 ± 4		
	exptl		108 ± 7[e]	1.491 16[f]	1172.6[g]	10.3[g]					
$1^2\Pi(1)$	CASSCF	62.39981	84.1	1.426	1349.0	10.6	1.51	6.61	0.620	−0.10	11.9
	MRCI	62.52850	90.5	1.417	1368.7	11.5	1.65	6.73	0.954	−0.20	10.5
	MRCI+Q	62.5359	90	1.417							10
	exptl[g]				1394.5	13.5					
$2^2\Sigma^-(1)$	CASSCF	62.36392	61.0	1.526	1104.2	10.0	1.66	6.59	1.39	−0.13	34.4
	MRCI	62.50594	76.3	1.503	1157.3	10.8	1.65	6.56	1.60	−0.17	24.7
	MRCI+Q	62.5153	78	1.502							23
$3^2\Delta(1)$	CASSCF	62.36657	62.4	1.529	1117.1	9.11	1.51	6.34	1.03	−0.10	32.7
	MRCI	62.50554	76.0	1.509	1150.8	9.90	1.58	6.49	1.17	−0.15	24.9
	MRCI+Q	62.5143	77	1.508							24
$4^4\Pi(1)$	CASSCF	62.37806	70.1	1.392	1478.0	9.43	1.51	6.63	−0.045	−0.06	25.5
	MRCI	62.50541	76.1	1.367	1548.5	8.46	1.45	6.46	0.316	−0.15	25.0
	MRCI+Q	62.5123	76	1.368							25
	exptl[g]				1574.8	13.9					24.60
$5^2\Sigma^+(1)$	CASSCF	62.35693	56.4	1.527	1098.2	9.33	1.48	6.62	1.05	−0.14	38.8
	MRCI	62.49060	66.6	1.508	1122.8	10.2	1.66	6.83	1.14	−0.14	34.3
	MRCI+Q	62.4984	67	1.508							34
	exptl[g]				1031.1						32.05[h]
$6^2\Pi(2)$	CASSCF	62.33672	44.6	1.665	864.7	7.92	1.35	6.38	−0.561	−0.15	51.5
	MRCI	62.47476	56.9	1.628	939.3	3.69	0.26	6.18	−0.604	0.00	44.2
	MRCI+Q	62.4844	58	1.627							43
$7^4\Sigma^-(2)$	CASSCF	62.33722	45.2	1.488	1248.3	22.1	2.37	5.88	−1.10	−0.14	51.2
	MRCI	62.46351	49.8	1.468	1265.4	2.45	1.513	6.33	−1.20	0.06	51.3
	MRCI+Q	62.4711	50	1.466							51
	exptl[f]			1.460 23							51.19
	exptl[g]				1289.6						51.33
	exptl[i]				1271(7)						51.49(2)
$8^2\Pi(3)$	CASSCF	62.31458	65.4	1.472					−0.101	−0.04	65.4
	MRCI	62.45282	72.3	1.440					0.081	−0.08	58.0
	MRCI+Q	62.4615	72	1.44							57
$9^2\Sigma^+(2)$	CASSCF	62.30824	60.8	1.335	1585.6	12.6	1.72	7.18	1.58	−0.11	69.3
	MRCI	62.44473	67.3	1.322	1722.3	7.47	4.56	6.57	1.76	−0.21	63.1
	MRCI+Q	62.4524	67	1.322							63
$10^2\Delta_G(2)$	CASSCF	62.25978	31.3	1.514	1052.1	16.8	2.35	7.59	−1.73	−0.18	99.7
	MRCI	62.40294	41.4	1.494	1121.5	18.0	2.20	7.25	−1.58	0.09	89.3
	MRCI+Q	62.4129	42	1.492							87
$10^2\Delta_L(2)$	MRCI	62.35431	10.9	2.514	236	26.7	−3.73	7.96		−0.01	119.8
	MRCI+Q	62.3641	12	2.55							118
$11^4\Delta(1)$	CASSCF	62.26711	0.31	1.921	435.8	26.1	2.78	10.1	−0.271	0.07	95.1
	MRCI	62.39665	7.80	1.856	555.1	18.8	2.65	8.14	−0.186	0.03	93.3
	MRCI+Q	62.4052	8.5	1.857							92
$12^6\Pi(1)$	CASSCF	62.28776	74.7	1.584	1063.7	7.88	1.29	5.68	−0.548	−0.08	82.2
	MRCI	62.39622	88.4	1.571	1077.0	8.09	1.31	5.80	−0.481	−0.07	93.5
	MRCI+Q	62.4014	89	1.574							95
$13^4\Sigma^+(1)$	CASSCF	62.26469	−1.21	1.941	405.4	30.7	3.61	11.6	−0.318	0.05	96.7
	MRCI	62.39384	6.03	1.871	530.2	21.6	2.87	8.48	−0.233	0.03	95.0
	MRCI+Q	62.4023	6.7	1.872							94
$14^2\Sigma^-_G(2)$	CASSCF	62.25949	2.48	1.868	491.3	20.6	2.48	9.89	−0.030	−0.13	99.9
	MRCI	62.39323	5.84	1.784	589.7	17.7	1.47	9.07	−0.051	0.00	95.4
	MRCI+Q	62.4026	6.6	1.780							94
$14^2\Sigma^-_L(2)$	CASSCF	62.26562	1.37	3.688					0.100	0.00	96.1
	MRCI	62.38530	0.86	3.338	98.0	8.44	1.30	7.76	−0.195	0.00	100.4
	MRCI+Q	62.3931	0.67	3.344							100
$15^4\Pi(2)$	CASSCF	62.25296	−8.02	1.663	851.6	0.81	1.24	6.59	0.276	−0.11	104.0
	MRCI	62.38766	2.22	1.652	958.5		0.45	5.42	0.619	−0.11	98.9
	MRCI+Q	62.3972	3.5	1.654							97
	exptl[i]				971(24)						98.26(7)
$16^2\Pi_G(4)$	CASSCF	62.22296	8.93	1.396	1509.7	38.5	3.01	6.09	3.22	0.04	122.9
	MRCI	62.37246	22.0	1.385	1515.1	35.9	3.51	6.39	3.13	−0.12	108.4
	MRCI+Q	62.3831	23	1.39							106
$16^2\Pi_L(4)$	CASSCF	62.21030	0.98	1.64					0.874	−0.12	130.8
	MRCI	62.35437	10.7	1.62					0.976	−0.14	119.8
	MRCI+Q	62.3657	12	1.63							117

TABLE 2 (Continued)

State	Method	$-E$	D_e	r_e	ω_e	$\omega_e x_e$	α_e (10^{-2})	$\bar{D}_e$ (10^{-6})	μ	q_c	T_e
$17^4\Pi_G(3)$	CASSCF	62.21526	36.9	1.636	935.8	12.0	1.53	6.09	−0.629	−0.10	127.7
	MRCI	62.33988	53.8	1.599	1012.8	15.3	1.96	6.03	−0.449	−0.04	128.9
	MRCI+Q	62.3475	56	1.598							129
$17^4\Pi_L(3)$	CASSCF	62.18970	20.9	2.30					−0.247	0.00	143.7
	MRCI	62.30923	34.6	2.23					0.136	−0.06	148.1
	MRCI+Q	62.3179	37	2.23							147
$18^4\Sigma^-(3)$	CASSCF	62.19700	25.8	2.205	784.2	16.2	0.06	1.43	0.323	−0.02	139.1
	MRCI	62.32534	44.9	2.077	730.5	16.9	−1.02	2.37	0.574	−0.04	138.0
	MRCI+Q	62.3360	49	2.040							136
$19^4\Sigma^+(2)$	CASSCF	62.19100	22.3	1.548	977.2	15.9	2.24	7.70	0.495	−0.12	142.9
	MRCI	62.31563	38.7	1.510	1075.5	12.4	2.09	7.46	0.864	−0.11	144.1
	MRCI+Q	62.3230	40	1.510							144
$20^4\Phi(1)$	CASSCF	62.16994	45.3	1.595	1015.7	9.07	1.43	5.96	−0.284	−0.02	156.1
	MRCI	62.31105	65.8	1.583	1038.2	8.83	1.38	5.97	−0.151	−0.09	147.0
	MRCI+Q	62.3210	68	1.588							145
$21^4\Pi_G(4)$	CASSCF	62.17537	15.5	1.644	848.7	19.3	2.25	7.21	−0.421	0.00	152.7
	MRCI	62.30582	32.5	1.602	971.0	11.9	1.63	6.40	−0.341	−0.04	150.2
	MRCI+Q	62.3150	35	1.599							149
$21^4\Pi_L(4)$	CASSCF	62.17570	15.7	2.21					−0.393	0.05	152.5
	MRCI	62.29447	25.3	2.12					−0.243	0.06	157.4
	MRCI+Q	62.3042	28	2.12							156
$22^4\Delta_G(2)$	CASSCF	62.13940	−10.5	1.534	1029.0	18.4	1.99	7.36	0.449	−0.09	175.3
	MRCI	62.28467	19.2	1.506	1080.3	16.6	2.09	7.46	0.797	−0.12	163.5
	MRCI+Q	62.2959	23	1.506							161
$22^4\Delta_L(2)$	CASSCF	62.15650	0.25	2.594	198.5	30.6	3.66	8.77	−0.134	0.00	164. 6
	MRCI	62.27204	11.3	2.230	357.8	8.62	−0.45	6.47	−0.472	0.01	171.4
	MRCI+Q	62.2802	13	2.165							171
$23^6\Pi(2)$	CASSCF	62.15711	0.66	3.791	79.8	0.88	−0.77	5.62	−0.066	0.00	164.2
	MRCI	62.25439	0.24	3.689	41.2	5.05	1.78	23.0	−0.026	0.00	182.5
	MRCI+Q	62.2594	0.31	3.53							184
$24^6\Sigma^-(1)$	CASSCF	62.13754	−12.3	1.418	1484.1	10.5	1.30	5.65			176.4
	MRCI	62.24717	−4.31	1.424	1441.0	11.5	1.39	5.85			187.1
	MRCI+Q	62.2527	−3.9	1.43							188
$25^6\Sigma^+(1)$		repulsive									
$26^6\Sigma^+(2)$		repulsive									
$27^6\Delta(1)$		repulsive									
$28^6\Pi(3)$	MRCI	62.23508	0.39	3.373	80.4	7.84	3.23	10.9	−0.054	0.00	194.6
	MRCI+Q	62.2386	0.48	3.34							197
$29^6\Sigma^-(2)$		repulsive									

[a] Internally contracted MRCI. [b] Multireference Davidson correction, ref 19. [c] MRCI/aug-cc-pCV5Z level, ref 1. [d] Complete basis set limit, ref 1. [e] Reference 2. [f] Reference 3, $r_e = 1.49116(34)$ Å, and $r_e = 1.46023(29)$ Å for the $X^4\Sigma^-$ and $B^4\Sigma^-$ respectively; T_0 value. [g] Reference 9. [h] The energy gap refers to $d^2\Sigma^+ \leftarrow a^2\Pi$, or $5^2\Sigma^+(1) \leftarrow 1^2\Pi(1)$ in our notation, thus our corresponding value is 23.8 kcal/mol. [i] Reference 10, T_0 value.

Both the $9^2\Sigma^+$ (BC) and $14^2\Sigma^+$ (AlC) states correlate adiabatically to Z (B, Al; ^{2}P) + C (^{1}D) fragments. However, as a result of two consecutive avoided crossings (around 4.0 and 3.2 bohr, and 4.1 and 3.9 bohr for BC and AlC, respectively), the second of which imparts its character around the equilibrium region, the in situ atoms find themselves at Z (^{4}P, s^1p^2; 0) + C (^{3}P; 0) states, Figures 2 and 3. Guided by the main configuration and populations, we claim that the bonding is comprised of two π bonds and a weak σ interaction due to a small charge transfer from C to B or Al through the σ frame. The symmetry carrying electron is localized on the B and Al atoms. Pictorially,

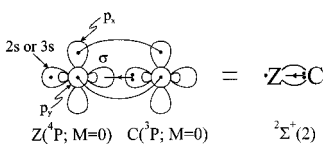

With respect to the adiabatic products, from Tables 2 and 3 we read, $D_e = 67.3$ (BC) and 21.1 (AlC) kcal/mol; with respect to the ground state atoms the D_e value of BC is 38.0 kcal/mol, but the AlC system is unbound.

$2^2\Sigma^-(1)$, $14^2\Sigma^-(2)/2^2\Sigma^-(1)$, and $10^2\Sigma^-(2)$. The two $^2\Sigma^-(1)$ states (BC, AlC) are of similar nature correlating to Z (^{2}P; ±1) + C (^{3}P; ∓1). As the following vbL diagram suggests

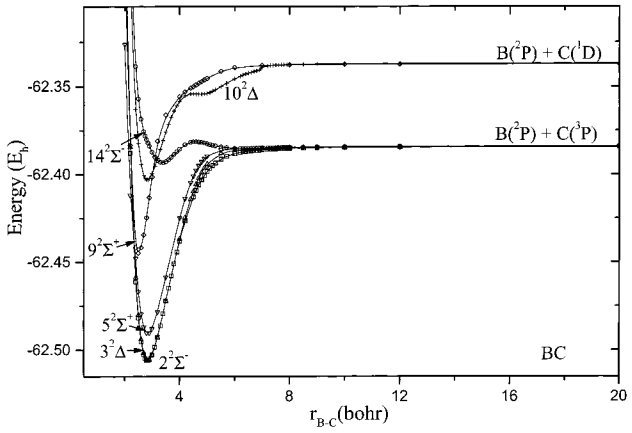

Figure 2. MRCI potential energy curves of doublets $2^2\Sigma^-(1)$, $3^2\Delta(1)$, $5^2\Sigma^+(1)$, $9^2\Sigma^+(2)$, $10^2\Delta(2)$, and $14^2\Sigma^-(2)$ of the BC molecule.

the Z (B, Al) + C atoms are held together by two $^1/_2\pi$ bonds and a weak $^1/_2\sigma$ interaction

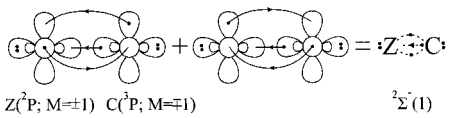

TABLE 3: Absolute Energies E (hartree), Dissociation Energies D_e (kcal/mol), Bond Distances r_e (Å), Harmonic Frequencies ω_e (cm^{-1}), First Anharmonic Corrections $\omega_e x_e$ (cm^{-1}), Rotational Vibrational Couplings α_e (cm^{-1}), Centrifugal Distortions $\bar{D}_e$(cm^{-1}), Dipole Moments μ (D), Mulliken Charges on the C Atom q_c, and Energy Gaps T_e (kcal/mol) for 31 States of the $^{27}Al^{12}C$ Molecule, at the CASSCF,[a] MRCI,[b] and MRCI+Q[c]/aug-cc-pVQZ Levels of Theory. "G" and "L" Subscripts Refer to Local and Global Minima

State	Method	$-E$	D_e	r_e	ω_e	$\omega_e x_e$	α_e (10^{-2})	$\bar{D}_e$ (10^{-6})	μ	q_c	T_e
$X^4\Sigma^-$	CASSCF	279.72717	68.6	1.976	650.8	3.84	0.48	1.33	1.22	−0.45	0.0
	MRCI	279.84015	77.9	1.970	649.1	4.22	0.50	1.36	1.74	−0.48	0.0
	MRCI+Q	279.8472	78.2	1.971							0.0
	exptl[d]		64.92		639.3	4.5					
	exptl[e]			1.955 03	654.84	4.293					
$1^2\Pi(1)$	CASSCF	279.67968	43.4	1.854	725.3	12.3	0.77	1.60	2.62	−0.42	29.8
	MRCI	279.80268	54.6	1.852	730.0	13.2	0.84	1.57	2.99	−0.48	23.5
	MRCI+Q	279.8110	55	1.855							23
$2^2\Sigma^-(1)$	CASSCF	279.67538	40.7	1.997	585.6	5.58	0.21	1.54	2.18	−0.38	32.5
	MRCI	279.79652	50.7	1.968	645.1	4.90	0.55	1.38	2.67	−0.48	27.4
	MRCI+Q	279.8051	51	1.972							26
$3^2\Delta(1)$	CASSCF	279.66808	35.3	1.971	658.0	16.9	0.95	1.32	1.70	−0.40	37.1
	MRCI	279.79383	48.9	1.979	643.1	5.45	0.54	1.34	1.96	−0.43	29.1
	MRCI+Q	279.8091	50	1.985							24
$4^2\Pi(2)$	CASSCF	279.66233	35.1	2.046	836.4	8.48	−0.012	0.65	1.86	−0.43	40.7
	MRCI	279.77996	40.6	2.040	769.5	5.10	0.072	0.79	1.80	−0.40	37.8
	MRCI+Q	279.7879	40	2.043							37
$5^2\Sigma^+(1)$	CASSCF	279.65531	27.3	1.972	638.1	25.6	1.24	1.40	1.72	−0.38	45.1
	MRCI	279.77467	36.9	1.989	619.3	6.39	0.606	1.41	1.89	−0.39	41.1
	MRCI+Q	279.7829	37	1.999							40
$6^4\Pi(1)$	CASSCF	279.64578	22.8	1.843	784.5	7.17	0.62	1.39	1.84	−0.36	51.1
	MRCI	279.75986	27.8	1.806	820.3	11.1	0.78	1.44	2.72	−0.45	50.4
	MRCI+Q	279.7673	28	1.805							50
$7^4\Sigma^-(2)$	CASSCF	279.61723	7.70	1.969	701.5	17.3	0.24	1.17	1.53	−0.43	69.0
	MRCI	279.73955	15.4	1.913	721.0	7.96	0.58	1.31	2.45	−0.44	63.1
	MRCI+Q	279.7482	15	1.916							62
	exptl[d]		38.64		746.2	10.3					64.65
	exptl[e]			1.894 16	733.93	7.60					64.12
$8^2\Pi(3)$	CASSCF	279.59916	22.0	1.888	639.9	6.04	0.78	1.85	1.96	−0.37	80.3
	MRCI	279.72222	33.4	1.858	630.5	10.9	1.18	2.05	2.38	−0.43	74.0
	MRCI+Q	279.7314	34	1.864							73
$9^4\Delta(1)$	CASSCF	279.61132	0.24	4.071					−0.154	0.00	72.7
	MRCI	279.71801	1.44	2.627					−0.831	0.03	76.6
	MRCI+Q	279.7265	2.0	2.55							76
$10^2\Sigma^-(2)$	CASSCF	279.60692	0.92	3.604					0.681	0.00	75.5
	MRCI	279.71733	1.35	3.759					−0.217	0.01	77.1
	MRCI+Q	279.7252	1.0	3.73							77
$11^4\Sigma^+(1)$	CASSCF	279.61106	0.07	4.451					−0.092	0.00	72.9
	MRCI	279.71684	0.71	3.3420					−0.469	0.02	77.4
	MRCI+Q	279.7248	1.0	2.775							77
$12^6\Pi(1)$	CASSCF	279.60950	63.7	1.956	691.6	4.23	0.46	1.25	0.671	−0.39	73.8
	MRCI	279.71079	74.9	1.953	687.6	3.94	0.46	1.28	0.841	−0.40	81.2
	MRCI+Q	279.7166	76	1.958							82
$13^4\Pi(2)$	CASSCF	279.58394	−14.9	2.010	614.7	5.92	0.62	1.46	1.51	−0.43	89.9
	MRCI	279.70996	−3.35	1.964	728.4	1.64	0.26	1.12	1.94	−0.41	81.7
	MRCI+Q	279.7215	−1.2	1.959							79
$14^2\Sigma^+(2)$	CASSCF	279.57888	7.57	1.753	837.6	11.3	0.66	1.64	3.24	−0.44	93.1
	MRCI	279.70282	21.1	1.753	808.9	33.4	1.48	1.77	3.22	−0.44	86.2
	MRCI+Q	279.7115	22	1.763							85
$15^2\Delta_G(2)$	CASSCF	279.57734	6.61	2.032	648.4	24.9	0.22	1.13	1.80	−0.36	94.0
	MRCI	279.70267	21.0	1.987	591.5	4.96	0.47	1.55	1.86	−0.41	86.3
	MRCI+Q	279.7131	23	1.976							84
$15^2\Delta_L(2)$	CASSCF	279.57122	2.77	2.737	163.6	2.48	−0.28	3.01	−0.277	−0.05	97.9
	MRCI	279.69017	13.1	2.937	272.7	1.78	−0.17	0.70	1.01	−0.10	94.1
	MRCI+Q	279.7027	17	2.98							91
$16^2\Pi(4)$	CASSCF	279.55367	7.60	1.974	599.1	5.16	0.60	1.57	1.15	−0.39	108.9
	MRCI	279.69059	14.7	1.936	677.5	9.02	0.67	1.39	1.67	−0.47	93.8
	MRCI+Q	279.7044	17	1.928							90
$17^2\Phi(1)$	CASSCF	279.54417	1.64	2.164	339.3	24.7	1.82	2.85	1.64	−0.33	114.8
	MRCI	279.68114	8.79	2.093	431.9	10.5	0.50	2.14	1.56	−0.35	99.8
	MRCI+Q	279.6939	10	2.085							96
$18^4\Sigma^-_G(3)$	CASSCF	279.54950	30.5	2.450	538.2	13.6	−0.083	0.54	0.771	−0.17	111.5
	MRCI	279.67417	46.2	2.328	389.7	2.92	−0.96	1.36	0.974	−0.22	104.2
	MRCI+Q	279.6902	52	2.25							99
$18^4\Sigma^-_L(3)$	MRCI	279.65790	35.9	3.575	176.4	5.03	−0.11	0.52	8.84	−0.58	114.4
$19^4\Pi_G(3)$	CASSCF	279.54186	26.2	2.012	584.2	6.97	0.64	1.48	0.525	−0.41	116.3
	MRCI	279.65815	36.6	1.982	638.9	4.25	0.50	1.35	0.843	−0.36	114.2
	MRCI+Q	279.6669	38	1.981							113

TABLE 3 (Continued)

State	Method	$-E$	D_e	r_e	ω_e	$\omega_e x_e$	α_e (10^{-2})	$\bar{D}_e$ (10^{-6})	μ	q_c	T_e
$19^4\Pi_L(3)$	CASSCF	279.54159	26.0	2.546	810.4	25.9	−0.076	0.18	−0.240	−0.04	116.5
	MRCI	279.65640	35.5	2.496	876.7	30.2	−0.28	0.18	0.108	−0.09	115.3
	MRCI+Q	279.6665	38	2.49							113
$20^4\Pi_G(4)$	CASSCF	279.52460	12.5	2.308	758.5	51.6	0.53	0.38	−0.447	−0.01	127.1
	MRCI	279.64278	32.3	2.265	1023.6	49.5	−0.34	0.24	0.574	−0.20	123.8
	MRCI+Q	279.6532	36	2.27							122
$20^4\Pi_L(4)$	CASSCF	279.51285	5.08	2.026	518.4	21.2	1.12	1.81	0.711	−0.30	134.5
	MRCI	279.63326	26.4	1.980	631.1	6.44	0.56	1.40	1.01	−0.38	129.8
	MRCI+Q	279.6445	30	1.98							127
$21^4\Phi(1)$	CASSCF	279.50837	44.1	1.963	674.1	4.21	0.48	1.29	1.09	−0.34	137.3
	MRCI	279.63875	60.4	1.974	653.9	4.13	0.50	1.33	0.971	−0.40	126.4
	MRCI+Q	279.6497	63	1.984							124
$22^4\Sigma^+(2)$	CASSCF	279.51111	3.33	1.967	653.7	43.6	0.11	1.38	0.484	−0.25	135.6
	MRCI	279.63216	25.8	1.905	640.0	3.50	0.82	1.72	1.44	−0.37	130.5
	MRCI+Q	279.6416	29	1.909							129
$23^6\Sigma^-(1)$	CASSCF	279.53082	15.1	1.913	665.6	12.6	0.88	1.54	1.53	−0.03	123.2
	MRCI	279.62124	18.9	1.914	645.9	10.4	0.87	1.63	1.71	−0.12	137.4
	MRCI+Q	279.6260	19	1.918							139
$24^4\Delta_G(2)$	CASSCF	279.506611	0.50	2.775	175.4	10.6	1.00	2.39	−0.168	0.05	138.4
	MRCI	279.61713	16.3	2.408	306.6	3.29	−0.16	1.82	−0.259	−0.12	139.9
	MRCI+Q	279.6281	20	2.340							137
$24^4\Delta_L(2)$	MRCI	279.61464	14.8	1.893	639.0	41.6	1.59	1.80	1.44	−0.40	141.5
	MRCI+Q	279.6294	21	1.921							137
$25^6\Pi(2)$	MRCI	279.59183	0.56	3.726	43.8	0.25	−0.26	7.31	−0.718	0.00	155.8
	MRCI+Q	279.5968	0.79	3.59							157
$26^6\Sigma^+(1)$		repulsive									
$27^6\Delta(1)$		repulsive									
$28^6\Sigma^+(2)$		repulsive									
$29^6\Pi(3)$	MRCI	279.56668	0.61	3.632	76.8	7.48	1.86	2.65	−0.048	0.00	171.6
	MRCI+Q	279.5713	0.96	3.59							173.1
$30^6\Sigma^-(2)$		repulsive									

[a] Nine active orbitals. [b] Internally contracted MRCI. [c] Multireference Davidson correction, ref 19. [d] Reference 4; D_e values calculated by the Birge−Sponer extrapolation method. [e] Reference 5.

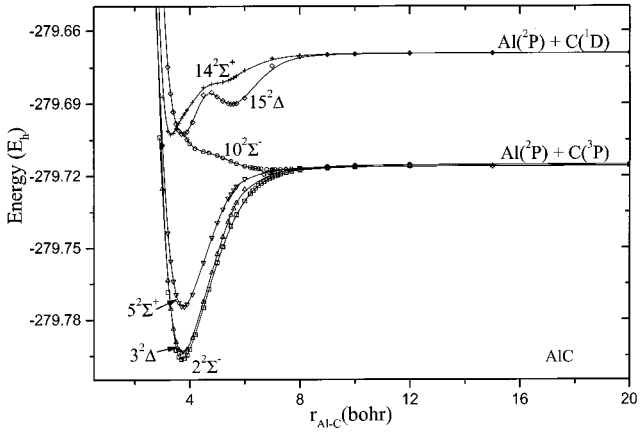

Figure 3. MRCI potential energy curves of doublets $2^2\Sigma^-(1)$, $3^2\Delta(1)$, $5^2\Sigma^+(1)$, $10^2\Sigma^-(2)$, $14^2\Sigma^+(2)$, and $15^2\Delta(2)$ of the AlC molecule.

Total equilibrium CASSCF Mulliken charges on C are 0.13 (BC) and 0.38 (AlC) e$^-$, transferred practically via the π frame. The D_e values are 76.3 (BC) and 50.7 (AlC) kcal/mol at the MRCI level of theory.

In the $14^2\Sigma^-(2)$ state of the BC molecule correlating to B (^{2}P; 0) + C (^{3}P; 0), we have a very shallow (local) minimum of 0.9 kcal/mol at the distance of 6.31 bohr, Figure 2. At about 4.5 bohr this state suffers an avoided crossing with an incoming (not calculated) $^2\Sigma^-(3)$ state correlating to B (^{2}P; ±1) + C (^{1}D; ∓1), resulting to a 1.6 kcal/mol (with respect to the asymptote) energy barrier, and a (global) minimum of D_e = 5.8 kcal/mol at r_e = 1.784 Å. A second avoided crossing occurs in the repulsive region of the PEC around 3 bohr with the repulsive part of the $^2\Sigma^-(3)$ state, imparting a B (^{4}P; ±1) + C (^{3}P; ∓1) character to the repulsive region of the $14^2\Sigma^-(2)$ state, as a result of a previous avoided crossing of the $^2\Sigma^-(3)$ state between 4.5 − 3.0 bohr, possibly with a $^2\Sigma^-(4)$ state.

The $10^2\Sigma^-(2)$ AlC state can be characterized as, essentially, repulsive, Figure 3. It shows a shallow minimum of 1.35 kcal/mol at 3.76 Å and an avoided crossing around 4.5 bohr with a $^2\Sigma^-(3)$ state correlating to the Al (^{4}P; ±1) + C (^{3}P; ∓1) atomic states.

$1^2\Pi(1)$, $6^2\Pi(2)$, $8^2\Pi(3)$, $16^2\Pi(4)/1^2\Pi(1)$, $4^2\Pi(2)$, $8^2\Pi(3)$, and $16^2\Pi(4)$. The BC and AlC $1^2\Pi(1)$ states correlate to Z (^{2}P; 0) + C (^{3}P; ±1), Z = B or Al, and they are the first excited states with T_e = 10.5 and 23.5 kcal/mol for BC and AlC, respectively (Tables 2 and 3). Both PECs, Figures 4 and 5, show avoided crossings around 4 bohr with the $6^2\Pi(2)$ (BC), and $4^2\Pi(2)$ (AlC) states, resulting to a flip of the M values, M = (0, ±1) to (±1, 0) after the crossing. According to the leading CFs and density distributions the bonding is clearly described by the vbL icon (B_1 component)

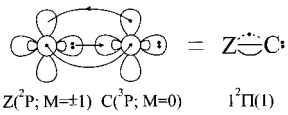

implying $^3/_2\pi$ and one σ bond. A net charge of 0.2 (BC) and 0.5 (AlC) e$^-$ migrate to the C atom. At r_e = 1.418 (BC) and 1.852 (AlC) Å, about 0.1 Å shorter than the $X^4\Sigma^-$ state(s), D_e = 90.5 (BC) and 54.6 (AlC) kcal/mol. For the BC species we obtain ω_e = 1368.7 cm^{-1}, in fair agreement with the experimental value ($a^2\Pi$)[9] of 1394.5 cm^{-1}; calculated and experimental[9] $\omega_e x_e$ values are 11.5 and 13.5 cm^{-1}, respectively (Table 2).

The next pair of analogous structures are the $6^2\Pi(2)$ (BC) and $4^2\Pi(2)$ (AlC) states, correlating to Z (^{2}P; ±1) + C (^{3}P; 0)

TABLE 4: Asymptotic Fragments, Dominant Equilibrium CASSCF CFs, and Mulliken Atomic Populations of the 30 Studied States of the BC Molecule

State	Asymptotic Fragments[a]	Dominant equilibrium CASSCF CFs (valence electrons only)	Equilibrium Mulliken atomic populations					
			B			C		
			2s	$2p_z$	$2p_x$[b]	2s	$2p_z$	$2p_x$[b]
$X^4\Sigma^-$	$\|^2P;0\rangle\|^3P;0\rangle$	$0.95\|1\sigma^2 2\sigma^2 3\sigma^1 1\pi_x^1 1\pi_y^1\rangle = \|A_2\rangle$	1.36	0.67	0.37	1.69	1.16	0.63
$1^2\Pi(1)$	$\|^2P;0\rangle\|^3P;\pm1\rangle$	$1/\sqrt{2}\|(0.841\sigma^2 2\sigma^2 - 0.351\sigma^2 3\sigma^2)(1\pi_x^1 1\pi_y^2 + 1\pi_x^2 1\pi_y^1)\rangle = \|B_1\rangle + \|B_2\rangle$	1.13	0.48	0.56	1.54	0.77	0.91[c]
$2^2\Sigma^-(1)$	$\|^2P;\pm1\rangle\|^3P;\mp1\rangle$	$0.80\|1\sigma^2 2\sigma^2 3\sigma^1 1\bar{\pi}_x^1 1\pi_y^1\rangle + 0.46\|1\sigma^2 2\sigma^2 3\sigma^1 1\pi_x^1 1\bar{\pi}_y^1\rangle = \|A_2\rangle$[c]	1.38	0.60	0.41	1.70	1.18	0.60
$3^2\Delta(1)$	$\|^2P;\pm1\rangle\|^3P;\pm1\rangle$	$1/\sqrt{2}0.66\|1\sigma^2 2\sigma^2 3\sigma^1(1\pi_x^2 - 1\pi_y^2 + 1\pi_x^1 1\bar{\pi}_y^1 - 1\bar{\pi}_x^1 1\pi_y^1)\rangle = \|A_1\rangle + \|A_2\rangle$	1.42	0.69	0.36	1.63	1.14	0.64
$4^4\Pi(1)$	$\|^2P;\pm1\rangle\|^3P;0\rangle$	$1/\sqrt{2}0.97\|1\sigma^2 2\sigma^1 3\sigma^1(1\pi_x^1 1\pi_y^2 + 1\pi_x^2 1\pi_y^1)\rangle = \|B_1\rangle + \|B_2\rangle$	1.03	0.62	0.62	1.46	0.86	0.86
$5^2\Sigma^+(1)$	$\|^2P;\pm1\rangle\|^3P;\mp1\rangle$	$0.64\|1\sigma^2 2\sigma^2 3\sigma^1(1\pi_x^2 + 1\pi_y^2)\rangle = \|A_1\rangle$	1.38	0.60	0.41	1.71	1.18	0.60
$6^2\Pi(2)$	$\|^2P;\pm1\rangle\|^3P;0\rangle$	$1/\sqrt{2}0.92\|1\sigma^2 2\sigma^2 3\sigma^2(1\pi_x^1 + 1\pi_y^1)\rangle = \|B_1\rangle + \|B_2\rangle$	1.82	0.77	0.16	1.65	1.38	0.46[c]
$7^4\Sigma^-(2)$	$\|^2P;\pm1\rangle\|^3P;\mp1\rangle$	$0.84\|1\sigma^2 2\sigma^1 3\sigma^2 1\pi_x^1 1\pi_y^1\rangle - 0.26\|1\sigma^2 2\sigma^2 3\sigma^1(1\pi_x^1 2\pi_y^1 + 2\pi_x^1 1\pi_y^1)\rangle - 0.24\|1\sigma^2 2\sigma^2 3\sigma^1 1\pi_x^1 1\pi_y^1\rangle = \|A_2\rangle$	1.42	0.64	0.37	1.67	1.13	0.66
$8^2\Pi(3)$	$\|^2P;\pm1\rangle\|^1D;0\rangle$	$1/\sqrt{2}[0.73\|1\sigma^2 2\sigma^1 3\sigma^1(1\bar{\pi}_x^1 1\pi_y^2 + 1\pi_x^2 1\bar{\pi}_y^1)\rangle + 0.50\|1\sigma^2 2\sigma^2 3\sigma^2(1\pi_x^1 + 1\pi_y^1)\rangle]^c = \|B_1\rangle + \|B_2\rangle$	1.09	0.62	0.55	1.47	0.95	0.83
$9^2\Sigma^+(2)$	$\|^2P;\pm1\rangle\|^1D;\mp1\rangle$	$0.90\|1\sigma^2 2\sigma^1 1\pi_x^2 1\pi_y^2\rangle = \|A_1\rangle$	0.84	0.25	0.83	1.34	0.62	1.09[c]
$10^2\Delta_G(2)$	$\|^2P;\pm1\rangle\|^1D;\pm1\rangle$	$1/\sqrt{2}0.62\|1\sigma^2 2\sigma^1 3\sigma^2(1\pi_x^2 - 1\pi_y^2 + 1\pi_x^1 1\bar{\pi}_y^1 - 1\bar{\pi}_x^1 1\pi_y^1)\rangle = \|A_1\rangle + \|A_2\rangle$	1.43	0.63	0.34	1.69	1.12	0.66
$10^2\Delta_L(2)$		$1/\sqrt{2}[0.46\|1\sigma^2 2\sigma^2 3\bar{\sigma}^1(1\pi_y^1 2\pi_y^1 - 1\pi_x^1 2\pi_x^1 - 1\pi_x^1 2\pi_y^1 + 2\pi_x^1 1\pi_y^1)\rangle + 0.31\|1\sigma^2 2\sigma^2 3\sigma^1(1\pi_x^1 2\bar{\pi}_x^1 - 1\pi_y^1 2\bar{\pi}_y^1 + 1\pi_x^1 2\bar{\pi}_y^1 - 2\bar{\pi}_x^1 1\pi_y^1)\rangle) + 0.23\|1\sigma^2 2\sigma^2 4\sigma^1(1\pi_y^2 - 1\pi_x^2 - 1\pi_x^1 1\bar{\pi}_y^1 + 1\bar{\pi}_x^1 1\pi_y^1)\rangle = \|A_1\rangle + \|A_2\rangle$	1.83	0.39	0.37	1.91	0.72	0.68
$11^4\Delta(1)$	$\|^2P;\pm1\rangle\|^3P;\pm1\rangle$	$1/\sqrt{2}0.67\|1\sigma^2 2\sigma^2 3\sigma^1(1\pi_x^1 2\pi_x^1 - 1\pi_y^1 2\pi_y^1 + 1\pi_x^1 2\pi_y^1 - 2\pi_x^1 1\pi_y^1)\rangle = \|A_1\rangle + \|A_2\rangle$	1.46	0.48	0.51	1.79	1.09	0.52[c]
$12^6\Pi(1)$	$\|^4P;\pm1\rangle\|^3P;0\rangle$	$1/\sqrt{2}0.99\|1\sigma^2 2\sigma^1 3\sigma^1(1\pi_x^1 1\pi_y^1 2\pi_y^1 + 1\pi_x^1 2\pi_x^1 1\pi_y^1)\rangle = \|B_1\rangle + \|B_2\rangle$	1.06	0.61	0.60	1.43	0.85	0.88
$13^4\Sigma^+(1)$	$\|^2P;\pm1\rangle\|^3P;\mp1\rangle$	$0.67\|1\sigma^2 2\sigma^2 3\sigma^1(1\pi_x^1 2\pi_x^1 + 1\pi_y^1 2\pi_y^1)\rangle = \|A_1\rangle$	1.55	0.44	0.52	1.85	1.03	0.52
$14^2\Sigma^-_G(2)$	$\|^2P;0\rangle\|^3P;0\rangle$	$0.49\|1\sigma^2 2\sigma^2 3\sigma^1(1\bar{\pi}_x^1 2\pi_y^1 + 2\pi_x^1 1\bar{\pi}_y^1)\rangle - 0.41\|1\sigma^2 2\sigma^2 3\sigma^1(1\pi_x^1 2\bar{\pi}_y^1 + 2\bar{\pi}_x^1 1\pi_y^1)\rangle + 0.21\|1\sigma^2 2\bar{\sigma}^1 3\sigma^2 1\pi_x^1 1\pi_y^1\rangle = \|A_2\rangle$	1.61	0.61	0.30	1.80	0.85	0.72
$14^2\Sigma^-_L(2)$		$0.73\|1\sigma^2 2\sigma^2 4\bar{\sigma}^1 1\pi_x^1 1\pi_y^1\rangle - 0.37\|1\sigma^2 2\sigma^2 4\sigma^1(1\pi_x^1 1\bar{\pi}_y^1 + 1\bar{\pi}_x^1 1\pi_y^1)\rangle = \|A_2\rangle$	1.89	0.06	0.53	1.96	1.00	0.52
$15^4\Pi(2)$	$\|^2P;0\rangle\|^3P;\pm1\rangle$	$1/\sqrt{2}[0.81\|1\sigma^2 2\sigma^2(1\pi_x^1 1\pi_y^1 2\pi_y^1 + 1\pi_x^1 2\pi_x^1 1\pi_y^1)\rangle + 0.36\|1\sigma^2 2\sigma^1 3\sigma^1(1\pi_x^1 1\pi_y^2 + 1\pi_x^2 1\pi_y^1)\rangle] = \|B_1\rangle + \|B_2\rangle$	1.07	0.60	0.58	1.47	0.81	0.90
$16^2\Pi_G(4)$	$\|^2P;\pm1\rangle\|^1D;\mp2\rangle$	$1/\sqrt{2}[\|1\sigma^2 2\sigma^2(0.59(2\pi_x^1 1\pi_y^2 + 1\pi_x^2 2\pi_y^1) + 0.17(1\pi_x^1 1\pi_y^1 2\bar{\pi}_y^1 + 1\pi_x^1 2\bar{\pi}_x^1 1\pi_y^1))\rangle - 0.32\|1\sigma^2 2\sigma^1 3\bar{\sigma}^1(1\pi_x^1 1\pi_y^2 + 1\pi_x^2 1\pi_y^1)\rangle - \|1\sigma^2 2\sigma^1 3\sigma^1(0.18(1\bar{\pi}_x^1 1\bar{\pi}_y^1 2\pi_y^1 + 1\bar{\pi}_x^1 2\pi_x^1 1\bar{\pi}_y^1) + 0.17(1\bar{\pi}_x^1 1\pi_y^2 + 1\pi_x^2 1\bar{\pi}_y^1))\rangle = \|B_1\rangle + \|B_2\rangle$	1.07	0.60	0.58	1.42	0.91	0.87
$16^2\Pi_L(4)$		$1/\sqrt{2}\|1\sigma^2 2\sigma^2(0.44(2\pi_x^1 1\pi_y^2 + 1\pi_x^2 2\pi_y^1) + 0.42(1\bar{\pi}_x^1 1\pi_y^1 2\pi_y^1 + 1\pi_x^1 2\pi_x^1 1\bar{\pi}_y^1) - 0.31(1\pi_x^1 1\pi_y^1 2\bar{\pi}_y^1 + 1\pi_x^1 2\bar{\pi}_x^1 1\pi_y^1))\rangle + 0.41\|1\sigma^2 2\sigma^1 3\sigma^1(1\bar{\pi}_x^1 1\pi_y^2 + 1\pi_x^2 1\bar{\pi}_y^1)\rangle^c = \|B_1\rangle + \|B_2\rangle$	1.05	0.51	0.98	1.56	0.84	0.50
$17^4\Pi_G(3)$	$\|^4P;\pm1\rangle\|^3P;0\rangle$	$1/\sqrt{2}\|1\sigma^2 2\sigma^1 3\sigma^1(0.57(1\bar{\pi}_x^1 1\pi_y^1 2\pi_y^1 + 1\pi_x^1 2\pi_x^1 1\bar{\pi}_y^1) + 0.54(2\pi_x^1 1\pi_y^2 + 1\pi_x^2 2\pi_y^1) = \|B_1\rangle + \|B_2\rangle$	1.25	0.40	0.61	1.65	0.64	0.88
$17^4\Pi_L(3)$		$1/\sqrt{2}[0.57\|1\sigma^2 2\sigma^1 3\sigma^1(1\pi_x^1 1\pi_y^2 + 1\pi_x^2 1\pi_y^1)\rangle - 0.29\|1\sigma^2 2\sigma^2 3\sigma^1 4\sigma^1(1\pi_x^1 + 1\pi_y^1)\rangle - 0.29\|1\sigma^2 2\sigma^1 3\sigma^1(1\pi_x^1 1\bar{\pi}_y^1 2\pi_y^1 + 1\bar{\pi}_x^1 2\pi_x^1 1\pi_y^1)\rangle + 0.27\|1\sigma^2 2\sigma^1 3\sigma^1(1\pi_x^1 1\pi_y^1 2\bar{\pi}_y^1 + 1\pi_x^1 2\bar{\pi}_x^1 1\pi_y^1)\rangle] = \|B_1\rangle + \|B_2\rangle$	1.48	0.72	0.39	1.75	0.79	0.73
$18^4\Sigma^-(3)$	$\|^4P;\pm1\rangle\|^3P;\mp1\rangle$	$\|(0.541\sigma^2 2\sigma^1 3\sigma^2 - 0.521\sigma^2 2\sigma^2 4\sigma^1)1\pi_x^1 1\pi_y^1\rangle - 0.27\|1\sigma^2 2\sigma^1 3\sigma^2(1\pi_x^1 2\pi_y^1 + 2\pi_x^1 1\pi_y^1)\rangle^c = \|A_2\rangle$	1.62	0.58	0.36	1.77	0.93	0.68
$19^4\Sigma^+(2)$	$\|^4P;\pm1\rangle\|^3P;\mp1\rangle$	$0.64\|1\sigma^2 2\sigma^1(1\pi_x^2 1\pi_y^1 2\pi_y^1 + 1\pi_x^1 2\pi_x^1 1\pi_y^2)\rangle = \|A_1\rangle$	0.85	0.17	0.90	1.43	0.52	1.04[c]
$20^4\Phi(1)$	$\|^4P;\pm1\rangle\|^1D;\pm2\rangle$	$1/\sqrt{2}0.50\|1\sigma^2 2\sigma^1 3\sigma^1(1\pi_x^2 2\pi_x^1 + 1\pi_y^2 2\pi_y^1 - 2\pi_x^1 1\pi_y^2 - 1\pi_x^2 2\pi_y^1 - 1\pi_x^1 1\bar{\pi}_y^1 2\pi_y^1 - 1\bar{\pi}_x^1 2\pi_x^1 1\pi_y^1 + 1\bar{\pi}_x^1 1\pi_y^1 2\pi_y^1 + 1\pi_x^1 2\pi_x^1 1\bar{\pi}_y^1)\rangle = \|B_1\rangle + \|B_2\rangle$	1.03	0.52	0.69	1.54	0.86	0.79
$21^4\Pi_G(4)$	$\|^4P;0\rangle\|^3P;\pm1\rangle$	$1/\sqrt{2}[\|(0.601\sigma^2 2\sigma^1 3\bar{\sigma}^1 + 0.321\sigma^2 2\bar{\sigma}^1 3\sigma^1)(1\pi_x^1 1\pi_y^1 2\pi_y^1 + 1\pi_x^1 2\pi_x^1 1\pi_y^1)\rangle - \|1\sigma^2 2\sigma^1 3\sigma^1(0.39(1\pi_x^1 1\bar{\pi}_y^1 2\,\pi_y^1 + 1\bar{\pi}_x^1 2\pi_x^1 1\pi_y^1) + 0.30(1\pi_x^1 1\pi_y^1 2\bar{\pi}_y^1 + 1\pi_x^1 2\,\bar{\pi}_x^1 1\pi_y^1))\rangle] = \|B_1\rangle + \|B_2\rangle$	1.04	0.52	0.70	1.54	0.85	0.81
$21^4\Pi_L(4)$		$1/\sqrt{2}[\|1\sigma^2 2\sigma^1 3\sigma^1(0.50(1\bar{\pi}_x^1 1\pi_y^1 2\pi_y^1 + 1\pi_x^1 2\pi_x^1 1\bar{\pi}_y^1) + 0.40(2\pi_x^1 1\pi_y^2 + 1\pi_x^2 2\pi_y^1))\rangle - \|(0.401\sigma^2 2\sigma^2 + 0.251\sigma^2 2\sigma^1 3\bar{\sigma}^1)(2\pi_x^1 1\pi_y^1 2\pi_y^1 + 1\pi_x^1 2\pi_x^1 2\pi_y^1)\rangle] = \|B_1\rangle + \|B_2\rangle$	1.12	0.36	0.76	1.74	0.75	0.71[c]
$22^4\Delta_G(2)$	$\|^4P;\pm1\rangle\|^3P;\pm1\rangle$	$1/\sqrt{2}0.65\|1\sigma^2 2\sigma^1(1\pi_x^2 1\pi_y^1 2\pi_y^1 - 1\pi_x^1 2\pi_x^1 1\pi_y^2 + 1\pi_x^2 2\pi_x^1 1\pi_y^1 - 1\pi_x^1 1\pi_y^2 2\pi_y^1)\rangle = \|A_1\rangle + \|A_2\rangle$	0.84	0.16	0.93	1.41	0.57	1.03
$22^4\Delta_L(2)$		$1/\sqrt{2}\|(0.441\sigma^2 2\sigma^1 3\sigma^2 - 0.321\sigma^2 2\sigma^2 4\sigma^1)(1\pi_x^1 2\pi_x^1 - 1\pi_y^1 2\pi_y^1 + 1\pi_x^1 2\pi_y^1 - 2\pi_x^1 1\pi_y^1)\rangle = \|A_1\rangle + \|A_2\rangle$	1.21	0.73	0.51	1.83	1.06	0.53[c]
$23^6\Pi(2)$	$\|^4P;0\rangle\|^3P;\pm1\rangle$	almost repulsive						
$24^6\Sigma^-(1)$	$\|^4P;\pm1\rangle\|^3P;\mp1\rangle$	$0.98\|1\sigma^2 2\sigma^1 3\sigma^1 4\sigma^1 1\pi_x^1 1\pi_y^1\rangle = \|A_2\rangle$[d]						
$25^6\Sigma^+(1)$	$\|^4P;0\rangle\|^3P;0\rangle$	repulsive						
$26^6\Sigma^+(2)$	$\|^4P;\pm1\rangle\|^3P;\mp1\rangle$	repulsive						
$27^6\Delta(1)$	$\|^4P;\pm1\rangle\|^3P;\pm1\rangle$	repulsive						
$28^6\Pi(3)$	$\|^2P;\pm1\rangle\|^5S\rangle$	almost repulsive						
$29^6\Sigma^-(2)$	$\|^2P;0\rangle\|^5S\rangle$	repulsive						

[a] $|^{2S+1}L;M\rangle_B$ $|^{2S+1}L;M\rangle_C$. [b] p_y populations are identical to p_x populations by symmetry. [c] MRCI values. [d] Problematic populations.

fragments. As was mentioned before, these states present avoided crossings with the BC/AlC $1^2\Pi(1)$ states, so their M equilibrium values become $(0, \pm1)$. In addition, in their repulsive part and around 2.7 (BC) and 3.3 (AlC) bohr, both PECs suffer

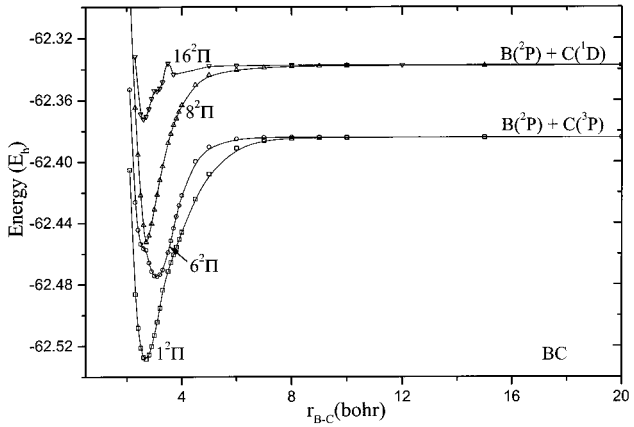

Figure 4. MRCI potential energy curves of doublets $1^2\Pi(1)$, $6^2\Pi(2)$, $8^2\Pi(3)$, and $16^2\Pi(4)$ of the BC molecule.

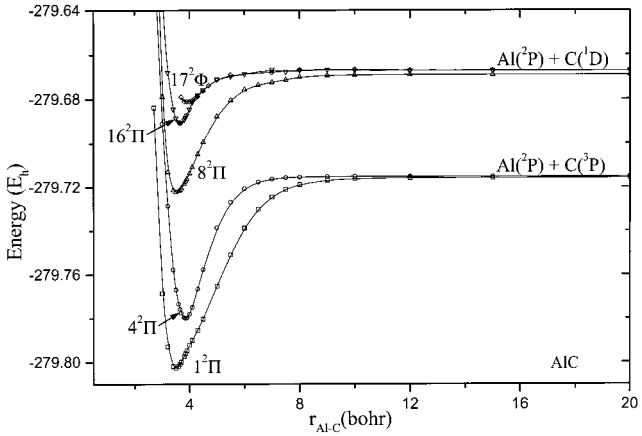

Figure 5. MRCI potential energy curves of doublets $1^2\Pi(1)$, $4^2\Pi(2)$, $8^2\Pi(3)$, $16^2\Pi(4)$, and $17^2\Phi(1)$ of the AlC molecule.

a second avoided crossing with the incoming $8^2\Pi(3)$ BC/AlC states (vide infra). This last avoided crossing shows clearly in the BC PEC, Figure 4. The bonding consists of $^1/_2\pi$ and one σ bond; pictorially (B_1 component)

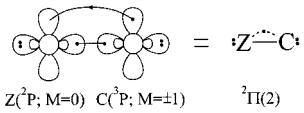

No net charge transfer is found in the BC system due to an approximately equal flux of e^- from C to B through the π frame, and from B to C through the σ frame. The AlC equilibrium populations are spurious due to the avoided crossing at 4 bohr (r_e = 3.855 bohr) with the $1^2\Pi(1)$ state (vide supra).

According to Tables 2 and 3, D_e = 56.9 and 40.6 kcal/mol for BC and AlC, respectively. Note the opposite dipole moment signs of BC and AlC.

Two out of the three possible $^2\Pi$ states which originate from Z (B, Al; ^{2}P) + C (^{1}D) fragments have been examined, namely, the $8^2\Pi(3)$ and $16^2\Pi(4)$ states, whose PECs are shown in Figures 4 and 5.

For the $8^2\Pi(3)$ state of BC the asymptotic products are described by the wave function $|^2P;\pm1\rangle|^1D;0\rangle$. Up to 3.2 bohr, the asymptotic character is maintained; between 3.2 and 2.7 bohr a character of B (^{4}P; ±1) + C (^{3}P; 0) is acquired owing to the interaction with the $16^2\Pi(4)$ state, while at the 2.7 bohr an avoided crossing occurs with the lower $6^2\Pi(2)$ state previously described. As a result the ensuing (approximate) minimum, r_e = 2.72 Å, entangles the characters B (^{4}P; ±1) + C (^{3}P; 0) (right PEC branch) and B (^{2}P; 0) + C (^{3}P; ±1) (left PEC branch). This is also clear from the dominant CFs participating at this point, Table 4. With respect to the formal minimum at the 2.72 Å a D_e = 72.3 kcal/mol is calculated; certainly, no meaningful spectroscopic constants can be given for this state.

Concerning the AlC $8^2\Pi(3)$ state the situation is similar to the one previously described, although there are some differences. In the interval 3.9 − 3.3 bohr, due to the interaction with the $16^2\Pi(4)$ state, the PEC carries the character of Al (^{4}P; ±1) + C (^{3}P; 0), with a clear minimum at 3.510 bohr (= 1.858 Å). In the repulsive part an avoided crossing occurs with the lower $4^2\Pi(2)$ state around 3.3 bohr. The bonding consists of $^3/_2\pi$ and $^1/_2\sigma$ bonds, with a net transfer of 0.4 e^- from Al to C atom, and D_e = 33.4 kcal/mol with respect to the asymptotic products, or 4.1 kcal/mol with respect to the ground-state atoms.

The rugged character of the BC $16^2\Pi(4)$ state, correlating to B (^{2}P; ±1) + C (^{1}D; ∓2), is due to the interactions of the $8^2\Pi(3)$ state (vide supra), a $^2\Pi(5)$ not calculated state correlating to the same fragments, and two more not calculated incoming $^2\Pi$ states ($^2\Pi(6)$, $^2\Pi(7)$) correlating to B (^{4}P) + C (^{3}P) fragments. The local (L) minimum at the 3.07 bohr (= 1.62 Å) seems to carry the character of the $8^2\Pi(3)$ state, while the in situ atoms at the global (G) minimum, r_e = 2.616 bohr (= 1.385 Å), are B (^{4}P; 0) + C (^{3}P; ±1), meaning that the G minimum correlates to the $^2\Pi(7)$ state. (See also Tables 4 and 2). With respect to the asymptotic products the $16^2\Pi_G(4)$ state has a binding energy of 22 kcal/mol, but its intrinsic bond strength, i.e., with respect to B (^{4}P) + C(^{3}P), is 22 + ΔE(B(^{4}P ← ^{2}P)) − ΔE(C(^{1}D ← ^{3}P)) = 75.6 kcal/mol. The bonding is comprised of $^3/_2\pi$ bonds and one σ bond.

Mutatis−mutandis the $16^2\Pi(4)$ PEC of AlC presents the same features as the $16^2\Pi(4)$ of BC although to a smaller extent, so it looks smoother at the MRCI level, Figure 5. However, the bonding consists of $^3/_2\pi$ bonds giving rise to a binding energy of 14.7 kcal/mol with respect to asymptotic products, or 14.7 + Δ*E*(Al(^{4}P ← ^{2}P)) − Δ*E*(C(^{1}D ← ^{3}P)) = 64.9 kcal/mol with respect to the Al (^{4}P) + C (^{3}P) atomic fragments.

$3^2\Delta(1)$, $10^2\Delta(2)/3^2\Delta(1)$, and $15^2\Delta(2)$. The $3^2\Delta(1)$ BC and AlC states, similar in every respect, correlate to Z (^{2}P; ±1) + C (^{3}P; ±1), Z = B or Al. The asymptotic character is maintained along the potential energy curve(s) for both molecules, Figures 2 and 3. According to the leading CASSCF equilibrium CFs and corresponding populations (Tables 4 and 5), the bonding is succinctly captured by the following vbL icons

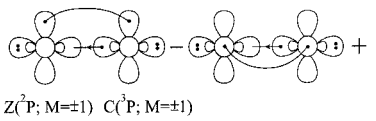

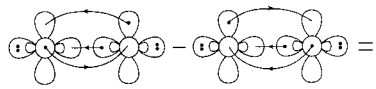

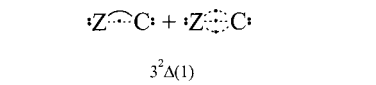

suggesting one π and $^1/_2\sigma$ bond. Notice that the symmetry of the first pair is A_1 and that of the second A_2. Along the σ frame about 0.2 e^- are moving from C to Z (B/Al), while along the π frame 0.3/0.6 e^-'s are migrating from B/Al to C. The MRCI D_e values are 76.0 (BC) and 48.9 (AlC) kcal/mol, Tables 2 and 3.

TABLE 5: Asymptotic Fragments, Dominant Equilibrium CASSCF CFs, and Mulliken Atomic Populations of the 31 Studied States of the AlC Molecule

State	Asymptotic Fragments[a]	Dominant equilibrium CASSCF CFs (valence electrons only)	Equilibrium Mulliken atomic populations					
			Al			C		
			3s	$3p_z$	$3p_x$[b]	2s	$2p_z$	$2p_x$[b]
$X^4\Sigma^-$	$\|^2P; 0\rangle\|^3P; 0\rangle$	$0.96\|1\sigma^2 2\sigma^2 3\sigma^1 1\pi_x^1 1\pi_y^1\rangle = \|A_2\rangle$	1.72	0.45	0.16	1.78	0.91	0.86
$1^2\Pi(1)$	$\|^2P; 0\rangle\|^3P; \pm1\rangle$	$1/\sqrt{2}\|(0.821\sigma^2 2\sigma^2 - 0.211\sigma^2 3\sigma^2)(1\pi_x^1 1\pi_y^2 + 1\pi_x^2 1\pi_y^1)\rangle = \|B_1\rangle + \|B_2\rangle$	1.39	0.27	0.39	1.73	0.56	1.04[c]
$2^2\Sigma^-(1)$	$\|^2P; \pm1\rangle\|^3P; \mp1\rangle$	$0.79\|1\sigma^2 2\sigma^2 3\sigma^1 1\bar{\pi}_x^1 1\pi_y^1\rangle + 0.46\|1\sigma^2 2\sigma^2 3\sigma^1 1\pi_x^1 1\bar{\pi}_y^1 = \|A_2\rangle$[c]	1.57	0.40	0.30	1.87	1.04	0.71
$3^2\Delta(1)$	$\|^2P; \pm1\rangle\|^3P; \pm1\rangle$	$1/\sqrt{2}0.67\|1\sigma^2 2\sigma^2 3\sigma^1(1\pi_x^2 - 1\pi_y^2 + 1\pi_x^1 1\bar{\pi}_y^1 - 1\bar{\pi}_x^1 1\pi_y^1)\rangle = \|A_1\rangle + \|A_2\rangle$	1.65	0.43	0.21	1.87	0.94	0.79
$4^2\Pi(2)$	$\|^2P; \pm1\rangle\|^3P; 0\rangle$	$1/\sqrt{2}[0.80\|1\sigma^2 2\sigma^2 3\sigma^2(1\pi_x^1 + 1\pi_y^1)\rangle + 0.39\|1\sigma^2 2\sigma^2(1\pi_x^1 1\pi_y^2 + 1\pi_x^2 1\pi_y^1)\rangle] = \|B_1\rangle + \|B_2\rangle$[d]						
$5^2\Sigma^+(1)$	$\|^2P; \pm1\rangle\|^3P; \mp1\rangle$	$0.65\|1\sigma^2 2\sigma^2 3\sigma^1(1\pi_x^2 + 1\pi_y^2)\rangle = \|A_1\rangle$	1.62	0.39	0.28	1.86	1.01	0.74
$6^4\Pi(1)$	$\|^2P; \pm1\rangle\|^3P; 0\rangle$	$1/\sqrt{2}0.80\|1\sigma^2 2\sigma^1 3\sigma^1(1\pi_x^1 1\pi_y^2 + 1\pi_x^2 1\pi_y^1)\rangle - 0.38\|1\sigma^2 2\sigma^2(1\pi_x^1 1\pi_y^1 2\pi_y^1 + 1\pi_x^1 2\pi_x^1 1\pi_y^1)\rangle = \|B_1\rangle + \|B_2\rangle$	1.09	0.40	0.55	1.64	0.81	0.93
$7^4\Sigma^-(2)$	$\|^2P; \pm1\rangle\|^3P; \mp1\rangle$	$0.69\|1\sigma^2 2\sigma^1 3\sigma^2 1\pi_x^1 1\pi_y^1\rangle + 0.39\|1\sigma^2 2\sigma^2 3\sigma^1(1\pi_x^1 2\pi_y^1 + 2\pi_x^1 1\pi_y^1)\rangle - 0.35\|1\sigma^2 2\sigma^2 3\sigma^1 1\pi_x^1 1\pi_y^1\rangle = \|A_2\rangle$	1.72	0.47	0.16	1.76	0.89	0.87
$8^2\Pi(3)$	$\|^2P; 0\rangle\|^1D; \pm1\rangle$	$1/\sqrt{2}[0.63\|1\sigma^2 2\sigma^1 3\sigma^1(1\bar{\pi}_x^1 1\pi_y^2 + 1\pi_x^2 1\bar{\pi}_y^1)\rangle + 0.35\|1\sigma^2 2\sigma^2(1\pi_x^1 1\pi_y^1 2\bar{\pi}_y^1 + 1\pi_x^1 2\bar{\pi}_x^1 1\pi_y^1)\rangle - 0.28.\|1\sigma^2 2\sigma^2(2\pi_x^1 1\pi_y^2 + 1\pi_x^2 2\pi_y^1)\rangle] = \|B_1\rangle + \|B_2\rangle$	1.08	0.35	0.52	1.72	0.77	0.93[c]
$9^4\Delta(1)$	$\|^2P; \pm1\rangle\|^3P; \pm1\rangle$	$1/\sqrt{2}0.65\|1\sigma^2 2\sigma^2 3\sigma^1(1\pi_x^1 2\pi_x^1 - 1\pi_y^1 2\pi_y^1 + 1\pi_x^1 2\pi_y^1 - 2\pi_x^1 1\pi_y^1)\rangle = \|A_1\rangle + \|A_2\rangle$	1.80	0.18	0.52	1.89	1.01	0.52[c]
$10^2\Sigma^-(2)$	$\|^2P; 0\rangle\|^3P; 0\rangle$	$0.65\|1\sigma^2 2\sigma^2 4\bar{\sigma}^1 1\pi_x^1 1\pi_y^1\rangle - 0.33\|1\sigma^2 2\sigma^2 4\sigma^1(1\pi_x^1 1\bar{\pi}_y^1 + 1\bar{\pi}_x^1 1\pi_y^1)\rangle + -0.30\|1\sigma^2 2\sigma^2 3\sigma^1 3\bar{\sigma}^1 1\pi_x^1 1\pi_y^1\rangle + 0.19\|1\sigma^2 2\sigma^2 3\sigma^1(1\pi_x^1 2\bar{\pi}_y^1 + 2\bar{\pi}_x^1 1\pi_y^1)\rangle = \|A_2\rangle$	1.92	0.13	0.45	1.94	0.93	0.56
$11^4\Sigma^+(1)$	$\|^2P; \pm1\rangle\|^3P; \mp1\rangle$	$0.64\|1\sigma^2 2\sigma^2 3\sigma^1(1\pi_x^1 2\pi_x^1 + 1\pi_y^1 2\pi_y^1)\rangle = \|A_1\rangle$	1.89	0.07	0.52	1.92	0.99	0.52
$12^6\Pi(1)$	$\|^4P; \pm1\rangle\|^3P; 0\rangle$	$1/\sqrt{2}\ 0.99\|1\sigma^2 2\sigma^1 3\sigma^1(1\pi_x^1 1\pi_y^1 2\pi_y^1 + 1\pi_x^1 2\pi_x^1 1\pi_y^1)\rangle = \|B_1\rangle + \|B_2\rangle$	1.03	0.43	0.53	1.58	0.89	0.94
$13^4\Pi(2)$	$\|^2P; 0\rangle\|^3P; \pm1\rangle$	$1/\sqrt{2}[0.73\|1\sigma^2 2\sigma^2(1\pi_x^1 1\pi_y^1 2\pi_y^1 + 1\pi_x^1 2\pi_x^1 1\pi_y^1)\rangle + 0.53\|1\sigma^2 2\sigma^1 3\sigma^1(1\pi_x^1 1\pi_y^2 + 1\pi_x^2 1\pi_y^1)\rangle] = \|B_1\rangle + \|B_2\rangle$	1.08	0.40	0.54	1.66	0.81	0.95
$14^2\Sigma^+(2)$	$\|^2P; \pm1\rangle\|^1D; \mp1\rangle$	$0.86\|1\sigma^2 2\sigma^1 1\pi_x^2 1\pi_y^2\rangle = \|A_1\rangle$	1.01	0.27	0.60	1.57	0.35	1.22[c]
$15^2\Delta_G(2)$	$\|^2P; \pm1\rangle\|^1D; \pm1\rangle$	$1/\sqrt{2}[0.54\|1\sigma^2 2\sigma^1 3\sigma^2(1\pi_x^2 - 1\pi_y^2 + 1\pi_x^1 1\bar{\pi}_y^1 - 1\bar{\pi}_x^1 1\pi_y^1)\rangle + 0.29\|1\sigma^2 2\sigma^2 3\sigma^1(1\bar{\pi}_x^1 2\pi_x^1 - 1\bar{\pi}_y^1 2\pi_y^1 + 1\bar{\pi}_x^1 2\pi_y^1 - 2\pi_x^1 1\bar{\pi}_y^1)\rangle] = \|A_1\rangle + \|A_2\rangle$	1.60	0.36	0.31	1.85	1.02	0.73
$15^2\Delta_L(2)$		$1/\sqrt{2}[0.51\|1\sigma^2 2\sigma^2 3\bar{\sigma}^1(1\pi_y^1 2\pi_y^1 - 1\pi_x^1 2\pi_x^1 + 2\pi_x^1 1\pi_y^1 - 1\pi_x^1 2\pi_y^1)\rangle + 0.30\|1\sigma^2 2\sigma^2 3\sigma^1(1\pi_x^1 2\bar{\pi}_x^1 - 1\pi_y^1 2\bar{\pi}_y^1 + 1\pi_x^1 2\bar{\pi}_y^1 - 2\bar{\pi}_x^1 1\pi_y^1)\rangle] = \|A_1\rangle + \|A_2\rangle$	1.80	0.18	0.44	1.89	0.94	0.60
$16^2\Pi(4)$	$\|^2P; \pm1\rangle\|^1D; \mp2\rangle$	$1/\sqrt{2}\ [\|(0.481\sigma^2 2\sigma^1 3\bar{\sigma}^1 - 0.41\sigma^2 2\bar{\sigma}^1 3\sigma^1 + 0.341\sigma^2 2\sigma^2)(1\pi_x^1 1\pi_y^2 + 1\pi_x^2 1\pi_y^1)\rangle + 0.33\|1\sigma^2 2\sigma^2(1\pi_x^1 1\pi_y^1 2\bar{\pi}_y^1 + 1\pi_x^1 2\bar{\pi}_x^1 1\pi_y^1)\rangle] = \|B_1\rangle + \|B_2\rangle$	1.08	0.30	0.58	1.75	0.80	0.90
$17^2\Phi(1)$	$\|^2P; \pm1\rangle\|^1D; \pm2\rangle$	$1/\sqrt{2} \times 0.48\|1\sigma^2 2\sigma^2(1\pi_x^2 2\pi_x^1 + 1\pi_y^2 2\pi_y^1 - 2\pi_x^1 1\pi_y^2 - 1\pi_x^2 2\pi_y^1 - 1\pi_x^1 1\bar{\pi}_y^1 2\pi_y^1 - 1\bar{\pi}_x^1 2\ \pi_x^1 1\pi_y^1 + 1\bar{\pi}_x^1 1\pi_y^1 2\pi_y^1 + 1\pi_x^1 2\pi_x^1 1\bar{\pi}_y^1\rangle = \|B_1\rangle + \|B_2\rangle$	1.18	0.23	0.60	1.81	0.73	0.89
$18^4\Sigma^-{}_G(3)$	$\|^2S\rangle\|^3P; 0\rangle$	$\|(0.571\sigma^2 2\sigma^2 4\sigma^1 - 0.491\sigma^2 2\sigma^1 3\sigma^2)1\pi_x^1 1\pi_y^1\rangle + 0.28\|1\sigma^2 2\sigma^2 3\sigma^1(1\pi_x^1 2\pi_y^1 + 2\pi_x^1 1\pi_y^1)\rangle$[c] $= \|A_2\rangle$	1.52	0.47	0.41	1.79	1.11	0.62
$18^4\Sigma^-{}_L(3)$		$\|(0.621\sigma^2 2\sigma^2 4\sigma^1 - 0.571\sigma^2 2\sigma^2 3\sigma^1)1\pi_x^1 1\pi_y^1\rangle = \|A_2\rangle$	1.88	0.72	0.06	1.87	0.72	0.97[c]
$19^4\Pi_G(3)$	$\|^2S\rangle\|^3P; \pm1\rangle$	$1/\sqrt{2}\|1\sigma^2 2\sigma^1 3\sigma^1(0.60(1\bar{\pi}_x^1 1\pi_y^1 2\pi_y^1 + 1\pi_x^1 2\pi_x^1 1\bar{\pi}_y^1) + 0.55(2\pi_x^1 1\pi_y^2 + 1\pi_x^2 2\pi_y^1) - 0.29(1\pi_x^1 1\pi_y^1 2\bar{\pi}_y^1 + 1\pi_x^1 2\bar{\pi}_x^1 1\pi_y^1)\rangle = \|B_1\rangle + \|B_2\rangle$[e]	1.27	0.27	0.54	1.79	0.63	0.95
$19^4\Pi_L(3)$		$1/\sqrt{2}[0.60\|1\sigma^2 2\sigma^2 3\sigma^1 4\sigma^1(1\pi_x^1 + 1\pi_y^1)\rangle + 0.45.\|1\sigma^2 2\sigma^1 3\sigma^1(1\pi_x^1 1\pi_y^2 + 1\pi_x^2 1\pi_y^1)\rangle] = \|B_1\rangle + \|B_2\rangle$[e]						
$20^4\Pi_G(4)$	$\|^4P; \pm1\rangle\|^3P; 0\rangle$	$1/\sqrt{2}[\|1\sigma^2 2\sigma^1 3\sigma^1(0.50(1\bar{\pi}_x^1 1\pi_y^1 2\pi_y^1 + 1\pi_x^1 2\pi_x^1 1\bar{\pi}_y^1) + 0.47(2\pi_x^1 1\pi_y^2 + 1\pi_x^2 2\pi_y^1))\rangle + 0.32\|1\sigma^2 2\sigma^2 3\sigma^1 4\sigma^1(1\pi_x^1 + 1\pi_y^1)\rangle] = \|B_1\rangle + \|B_2\rangle$[e]						
$20^4\Pi_L(4)$		$1/\sqrt{2}[\|(0.571\sigma^2 2\sigma^1 3\bar{\sigma}^1 + 0.351\sigma^2 2\bar{\sigma}^1 3\sigma^1)(1\pi_x^1 1\pi_y^1 2\pi_y^1 + 1\pi_x^1 2\pi_x^1 1\pi_y^1)\rangle - \|1\sigma^2 2\sigma^1 3\sigma^1(0.40(1\pi_x^1 1\bar{\pi}_y^1 2\pi_y^1 + 1\bar{\pi}_x^1 2\pi_x^1 1\pi_y^1) + 0.37(1\pi_x^1 1\pi_y^1 2\bar{\pi}_y^1 + 1\pi_x^1 2\bar{\pi}_x^1 1\pi_y^1))\rangle] = \|B_1\rangle + \|B_2\rangle$	0.98	0.36	0.68	1.74	0.88	0.82
$21^4\Phi(1)$	$\|^4P; \pm1\rangle\|^1D; \pm2\rangle$	$1/\sqrt{2}0.49\|1\sigma^2 2\sigma^1 3\sigma^1(1\pi_x^2 2\pi_x^1 + 1\pi_y^2 2\pi_y^1 - 2\pi_x^1 1\pi_y^2 - 1\pi_x^2 2\pi_y^1 - 1\pi_x^1 1\bar{\pi}_y^1 2\pi_y^1 - 1\bar{\pi}_x^1 2\pi_x^1 1\pi_y^1 + 1\bar{\pi}_x^1 1\pi_y^1 2\pi_y^1 + 1\pi_x^1 2\pi_x^1 1\bar{\pi}_y^1\rangle = \|B_1\rangle + \|B_2\rangle$	0.97	0.37	0.65	1.72	0.87	0.85
$22^4\Sigma^+(2)$	$\|^4P; \pm1\rangle\|^3P; \mp1\rangle$	$0.63\|1\sigma^2 2\sigma^1(1\pi_x^2 1\pi_y^1 2\pi_y^1 + 1\pi_x^1 2\pi_x^1 1\pi_y^2)\rangle = \|A_1\rangle$	0.91	0.12	0.75	1.66	0.34	1.14[c]
$23^6\Sigma^-(1)$	$\|^4P; \pm1\rangle\|^3P; \mp1\rangle$	$0.98\|1\sigma^2 2\sigma^1 3\sigma^1 4\sigma^1 1\pi_x^1 1\pi_y^1\rangle = \|A_2\rangle$	1.34	1.03	0.13	1.42	0.89	0.84[f]
$24^4\Delta_G(2)$	$\|^4P; \pm1\rangle\|^3P; \pm1\rangle$	$1/\sqrt{2}\|(0.491\sigma^2 2\sigma^1 3\sigma^2 - 0.291\sigma^2 2\sigma^2 4\sigma^1)(1\pi_x^1 2\pi_x^1 - 1\pi_y^1 2\pi_y^1 + 1\pi_x^1 2\pi_y^1 - 2\pi_x^1 1\pi_y^1)\rangle = \|A_1\rangle + \|A_2\rangle$	1.16	0.63	0.52	1.85	1.16	0.53[c]
$24^4\Delta_L(2)$		$1/\sqrt{2}0.59\|1\sigma^2 2\sigma^1(1\pi_x^2 1\pi_y^1 2\pi_y^1 - 1\pi_x^1 2\pi_x^1 1\pi_y^2 + 1\pi_x^2 2\pi_x^1 1\pi_y^1 - 1\pi_x^1 1\pi_y^2 2\pi_y^1)\rangle = \|A_1\rangle + \|A_2\rangle$	0.95	0.14	0.69	1.67	0.36	1.14[c]
$25^6\Pi(2)$	$\|^4P; 0\rangle\|^3P; \pm1\rangle$	almost repulsive						
$26^6\Sigma^+(1)$	$\|^4P; 0\rangle\|^3P; 0\rangle$	repulsive						
$27^6\Delta(1)$	$\|^4P; \pm1\rangle\|^3P; \pm1\rangle$	repulsive						
$28^6\Sigma^+(2)$	$\|^4P; \pm1\rangle\|^3P; \mp1\rangle$	repulsive						
$29^6\Pi(3)$	$\|^2P; \pm1\rangle\|^5S\rangle$	almost repulsive						
$30^6\Sigma^-(2)$	$\|^2P; 0\rangle\|^5S\rangle$	repulsive						

[a] $|^{2S+1}L;M\rangle_{Al}|^{2S+1}L;M\rangle_C$. [b] p_y populations are identical to p_x by symmetry. [c] MRCI values. [d] Problematic populations due to avoided crossing(s). [e] On the top of the avoided crossing. [f] 0.32 e^- are missing from the σ frame because the d_σ is occupied.

The 10 (BC) and $15^2\Delta(2)$ (AlC) states trace their lineage to Z (^2P; ±1) + C (^1D; ±1), Z = B or Al. At distances of 4.75 and 5.55 bohr, local (L) minima are observed corresponding to D_e = 10.9 and 13.1 kcal/mol for BC and AlC, respectively, Figures 2 and 3. Avoided crossings around 4.4 (BC) and 4.6 (AlC) bohr (Figures 2 and 3) with a (not calculated) $^2\Delta(3)$ state

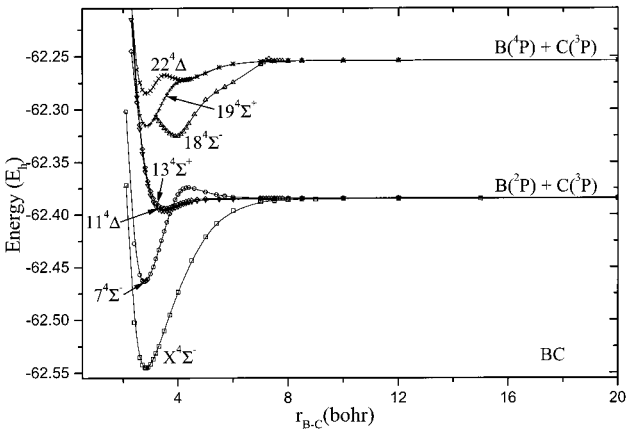

Figure 6. MRCI potential energy curves of quartets $X^4\Sigma^-$, $7^4\Sigma^-(2)$, $11^4\Delta(1)$, $13^4\Sigma^+(1)$, $18^4\Sigma^-(3)$, $19^4\Sigma^+(2)$, and $22^4\Delta(2)$ of the BC molecule.

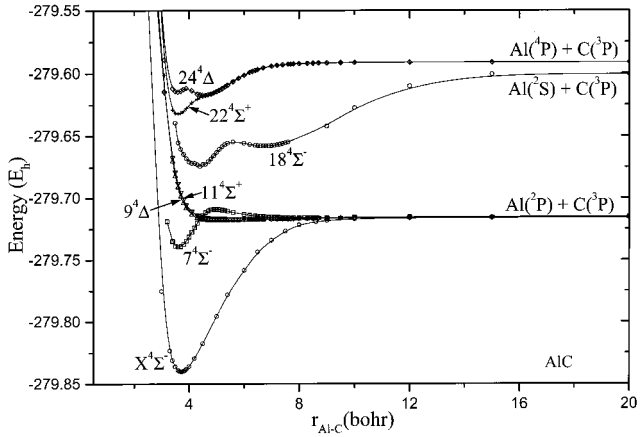

Figure 7. MRCI potential energy curves of quartets $X^4\Sigma^-$, $7^4\Sigma^-(2)$, $9^4\Delta(1)$, $11^4\Sigma^+(1)$, $18^4\Sigma^-(3)$, $22^4\Sigma^+(2)$, and $24^2\Delta(2)$ of the AlC molecule.

correlating to Z (^{4}P; ±1) + C (^{3}P; ±1), result in global (G) minima carrying the character of the $^2\Delta(3)$ state. Energy barriers measured from the L minima are 0.14 (BC) and 3.03 (AlC) kcal/mol.

At the G minima, r_e = (BC/AlC) = 1.4936/1.9872 Å, the bonding can be represented by the diagrams

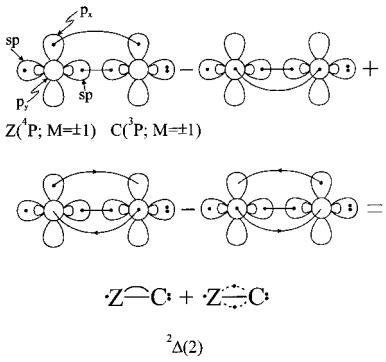

implying a σ and a π bond. The σ bond is due to the interaction of a strong hybrid on Z (B, Al) and the $2p_z$ orbital of the C atom, while along the π frame 0.3/0.5 e$^-$ are transferred from B/Al to the C atom. Note the opposite signs of dipole moments of the BC and AlC molecules, Tables 2 and 3. The binding energies with respect to the asymptotic products are D_e (BC/AlC) = 41.4/21.0 kcal/mol, but with respect to the diabatic fragments the corresponding values are 95.0/71.2 kcal/mol.

$17^2\Phi(1)$ AlC State. The asymptotic fragments are Al (^{2}P; ±1) + C (^{1}D; ±2). The fact that we need eight determinants (four of B_1 and four of B_2 symmetry, Table 3) to describe this state correctly, makes the bonding description with simple "chemical" terms uneconomical; D_e = 8.8 kcal/mol at the MRCI level.

3.2.b. Symmetries $^4\Sigma^+$, $^4\Sigma^-$, $^4\Pi$, $^4\Delta$, *and* $^4\Phi$. $13^4\Sigma^+(1)$, $19^4\Sigma^+(2)/11^4\Sigma^+(1)$, and $22^4\Sigma^+(2)$. The $13^4\Sigma^+(1)$ (BC) and $11^4\Sigma^+(1)$ (AlC) states, correlating to Z (^{2}P; ±1) + C (^{3}P; ∓1) fragments, are both unbound at the CASSCF and weakly bound at the MRCI level of theory, D_e (BC/AlC) = 6.03/0.71 kcal/mol, at r_e = 1.871/3.342 Å. In both systems the bonding consists of $^1/_2\sigma$ bond due to a slight charge transfer from the $2p_z$ C orbital to a $2s2p_z$ hybrid on the B atom, or to the $3p_z$ orbital of the Al atom. Corresponding PECs are shown in Figures 6 and 7.

The $19^4\Sigma^+(2)$ (BC) and $22^4\Sigma^+(2)$ (AlC) states trace their ancestry to Z (^{4}P; ±1) + C (^{3}P; ∓1) atomic fragments, Figures 6 and 7. Both states suffer avoided crossings around 4.4 bohr with another, not calculated, $^4\Sigma^+(3)$ state correlating either to Z (^{4}P; 0) + C (^{3}P; 0) or Z (^{4}P; 0) + C (^{1}D; 0). The C $|^3P;0\rangle$ and $|^1D;0\rangle$ states are described by the determinants $1/\sqrt{2}(p_x\bar{p}_y + \bar{p}_x p_y) = |A_2\rangle$ and $1/\sqrt{4}[p_x^2 + p_y^2 - i(p_x\bar{p}_y + \bar{p}_x p_y) = |A_1\rangle + |A_2\rangle$, respectively. These should be combined with the Z (^{4}P; 0) = $s^1p_x1p_y1$ determinant of A_2 symmetry. Because the molecular symmetry of the Σ^+ state should be of symmetry A_1, having not calculated the $^4\Sigma^+(3)$ state we cannot be sure where our $^4\Sigma^+(2)$ equilibrium states correlate diabatically. However, in either case the bond character will be the same, namely $|s^1p_x^1\,p_y^1\rangle|p_x\bar{p}_y + \bar{p}_x p_y\rangle$. The Z (B/Al) + C atoms are held together by $^1/_2\sigma$ "interaction" and one π bond, or pictorially

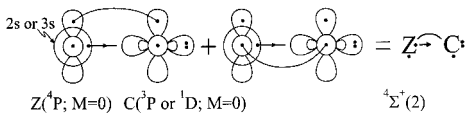

Over all, and practically through the π frame, about 0.1/0.4 e$^-$ are transferred from B/Al to C atom, respectively. The binding energy is D_e (BC/AlC) = 38.7/25.8 kcal/mol with respect to the adiabatic fragments at the MRCI level, Tables 2 and 3.

$X^4\Sigma^-(1)$, $7^4\Sigma^-(2)$, $18^4\Sigma^-(3)/X^4\Sigma^-(1)$, $7^4\Sigma^-(2)$, and $18^4\Sigma^-(3)$. As has been already mentioned in the Introduction the ground states for both molecules are of $^4\Sigma^-$ symmetry and they have been discussed extensively elsewhere.[1] Results concerning the $X^4\Sigma^-$ states are included in Tables 2 and 3 for reasons of comparison.

The next states of the same symmetry, namely, $7^4\Sigma^-(2)$, are 51.3 and 63.1 kcal/mol higher than the X states of BC and AlC, respectively. (Figures 6, 7 and Tables 2, 3). They correlate to Z (^{2}P; ±1) + C (^{3}P; ∓1), Z = B/Al; as we approach equilibrium they both experience avoided crossings around 4.3 (BC) and 5.1 (AlC) bohr with the $18^4\Sigma^-(3)$ state(s). As a result the minimum correlates to Z (^{4}P; ±1) + C (^{3}P; ∓1), Figures 6 and 7. The bonding can be clearly represented by the vbL icon

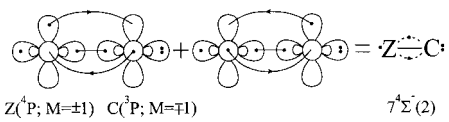

implying two $^1/_2\pi$ and one σ bond. Our CASSCF populations indicate that 0.2/0.3 e$^-$ are moving from C to Z (B/Al) along the σ route, while 0.3/0.7 e$^-$ through the π frame are migrating from Z (B/Al) to the C atom. Practically, no net transfer is observed in the BC system, but there is a net transfer of 0.4 e$^-$

to the C atom in the AlC molecule. Note the opposite signs of dipole moments between BC and AlC, Tables 2 and 3.

Existing experimental results for the $^4\Sigma^-(2)$ states confirm nicely the validity of our calculations. In particular, concerning the BC molecule (experimental numbers in parentheses) $r_e = 1.468$ (1.46023[3]) Å, $\omega_e = 1265.4$ (1289.6[9] and 1271(7)[10]) cm^{-1}, $T_e = 51.3$ (51.33[9] and $T_0 = 51.19$,[3] 51.49(2)[10]) kcal/mol. The 0.008 Å difference in bond length is due almost entirely to core−correlation effects as was proved in our previous work.[1] As a matter of fact, by including the core correlation in the $X^4\Sigma^-$ (BC) state, the bond length decreased by 0.006 Å at the corresponding complete basis set (CBS) limit. Assuming that the same bond length shortening is at work in the $^4\Sigma^-(2)$ state, our estimated bond length is in harmony with the experimental value. The rest of the experimental values are in excellent agreement with the theoretical findings, Table 2. Now, concerning the AlC system we report (Table 3): $r_e = 1.913$ (1.89416[5]) Å, $\omega_e = 721.0$ (746.2[4] and 733.93[5]) cm^{-1}, $\omega_e x_e = 7.96$ (10.3[4] and 7.60[5]) cm^{-1}, and $T_e = 63.1$ (64.65[4] and 64.12[5]) kcal/mol. Certainly, the same comments hold here as in BC as far as the bond length is concerned. At the MRCI level we obtain $D_e = 15.4$ kcal/mol with respect to Al (^{2}P) + C (^{3}P), in complete *disagreement* with the experimental value[4] of 38.64 kcal/mol. We believe that the latter is in error and we ascribe this result to the pitfalls of the Birge−Sponer[20] extrapolation used. Finally, the internal bond strength of AlC, i.e., with respect to Al (^{4}P) + C (^{3}P), is 15.4 + $\Delta E(^4P \leftarrow ^2P) = 94.8$ kcal/mol; corresponding values for BC are 49.8 and 132.7 kcal/mol.

Owing to the complexity of the BC and AlC $18^4\Sigma^-(3)$ PECs, we are forced to discuss them separately starting with the BC molecule, Figure 6. The BC $18^4\Sigma^-(3)$ state correlates to B (^{4}P; ±1) + C (^{3}P; ∓1); this character is conserved up to an interatomic distance of 7.5 bohr. Between 7.5 and 5 bohr it acquires the character of B (^{2}P;0) + C (^{5}S), due to an avoided crossing around 8 bohr with the (not calculated) $^4\Sigma^-(4)$ state. A second avoided crossing with the same state around 5 bohr reverts the $^4\Sigma^-(3)$ to its original character. A final avoided crossing at 4 bohr with the lower $^4\Sigma^-(2)$ state, discussed previously, creates a "minimum" at $r_e \approx 3.9$ bohr (≈2.1 Å), with $D_e = 44.9$ kcal/mol with respect to that minimum.

We now trace from infinity the AlC PEC, Al (^{2}S-Rydberg) + C (^{3}P; 0). This character is maintained up to 10 bohr. Around this region it suffers an avoided crossing with a, not calculated, $^4\Sigma^-(4)$ state, acquiring at this region the character Al (^{2}P; 0) + C (^{5}S), which is maintained up to 6 bohr, while at 6.75 bohr (≈ 3.75 Å) shows a local (L) minimum. The bonding at the L minimum consists of a σ bond between the $3p_z$ (Al) + 2s (C), enhanced by small π interactions and amounting to $D_e = 35.9$ kcal/mol. Remarkably, at the L minimum we calculate a dipole moment $\mu = 8.84$ D. A second avoided crossing with the $^4\Sigma^-(4)$ state again at 6 bohr correlating to Al (^{4}P; ±1) + C (^{3}P; ∓1), and finally a third one with the lower $^4\Sigma^-(2)$ at about 5 bohr (vide supra), results in a global (G) minimum at $r_e = 4.40$ bohr (= 2.33 Å) and $D_e = 46.2$ kcal/mol with respect to Al (^{2}S-Rydberg) + C (^{3}P) fragments.

$4^4\Pi(1)$, $15^4\Pi(2)$, $17^4\Pi(3)$, $21^4\Pi(4)/6^4\Pi(1)$, $13^4\Pi(2)$, $19^4\Pi(3)$, and $20^4\Pi(4)$. The first two $^4\Pi$ states, $4^4\Pi(1)$ and $6^4\Pi(1)$ for BC and AlC, respectively, correlate to Z (^{2}P; ±1) + C (^{3}P; 0), Z = B or Al. Following the PECs from infinity, Figures 8 and 9, a first avoided crossing is found at 3.5 (BC) and 3.8 (AlC) bohr with the $15^4\Pi(2)$ and $13^4\Pi(2)$ states, which correlate *diabatically* to Z (^{4}P; ±1) + C (^{3}P; 0). As a result the in situ "equilibrium" atoms Z (B/Al) and C carry this character, i.e., the $^4\Pi(1)$ states correlate diabatically to Z (^{4}P; ±1) + C (^{3}P; 0). In accordance with the leading CASSCF CFs and electron distributions the bonding is composed of $^3/_2\pi$ and $^1/_2\sigma$ bond, or, pictorially,

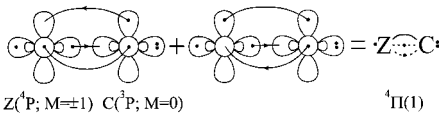

Along the σ frame, 0.32/0.45 e$^-$ are moving from B/Al to the hybrid carbon orbitals, $(sp)^{1.64 + 0.54}/(sp)^{1.64 + 0.36}$; along the π frame 0.25/0.1 e$^-$'s are transferred from C to B/Al. The net transfer is about 0.1/0.4 e$^-$ from B/Al to C atom. With respect to the ground-state fragments we calculate D_e (BC/AlC) = 76.1/27.8 kcal/mol or 159.0/107.2 kcal/mol with respect to Z (^{4}P) + C (^{3}P) (internal bond strength).

Experimental results for BC ($A^4\Pi$)[9] are $T_e = 24.60$ kcal/mol, $\omega_e = 1574.8$ cm^{-1}, and $\omega_e x_e = 13.9$ cm^{-1} in relative agreement with the MRCI theoretical values, viz., 25.0 kcal/mol, 1548.5, and 8.46 cm^{-1}.

We now examine the $15^4\Pi(2)$ (BC) and $13^4\Pi(2)$ (AlC) states, whose PECs are shown in Figures 8 and 9. Their character at infinity Z (^{2}P; 0) + C (^{3}P; ±1) is maintained up to 4.1 (BC) and 4.7 (AlC) bohr. Because of severe avoided crossings around these regions with the $^4\Pi(3)$ state(s), the PECs acquire the character of the latter, i.e., Z (^{4}P; ±1) + C (^{3}P; 0), continuing to the repulsive part of the curves as Z (^{2}P; ±1) + C (^{3}P; 0) due to the avoided crossings with the lower $^4\Pi(1)$ states (vide supra). The energy barrier heights measured from the resulting "minima" are 41.7 and 26.1 kcal/mol for BC and AlC,

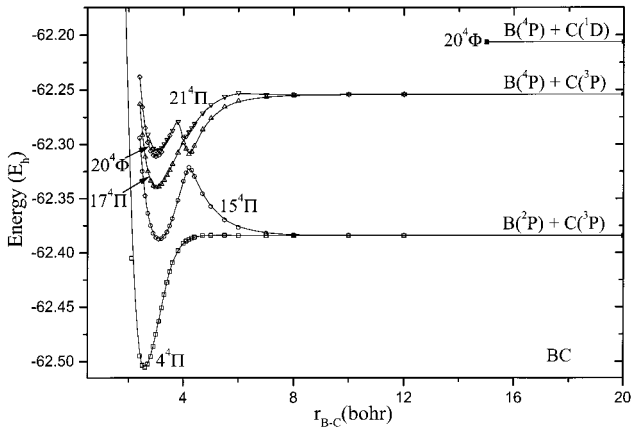

Figure 8. MRCI potential energy curves of quartets $4^4\Pi(1)$, $15^4\Pi(2)$, $17^4\Pi(3)$, $20^4\Phi(1)$, and $21^4\Pi(4)$ of the BC molecule.

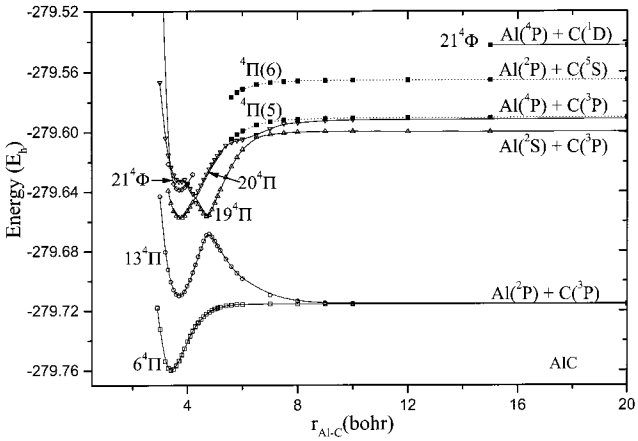

Figure 9. MRCI potential energy curves of quartets $6^4\Pi(1)$, $13^4\Pi(2)$, $19^2\Pi(3)$, $20^4\Pi(4)$, and $21^4\Phi(1)$ of the AlC molecule.

respectively. With respect to the ground-state atoms we obtain, r_e (BC/AlC) $\approx$ 3.12/3.71 bohr (= 1.65/1.96 Å), and MRCI D_e (BC/AlC) = 2.22/−3.35 kcal/mol, slightly bound and unbound, respectively.

Wyss et al.[10] studied the $^4\Pi(2)$ state of the BC by electronic absorption spectra in neon matrices and named this state as $C^4\Pi$. In our nomenclature this corresponds to the $E^4\Pi$ due to the intervening states $11^4\Delta(1)$ ($\equiv C^4\Delta$) and $13^4\Sigma^+(1)$ ($\equiv D^4\Sigma^+$), 5.6 and 3.9 kcal/mol lower than the $15^4\Pi(2)$ state. Our MRCI results, T_e (T_0) = 98.9 (98.6) kcal/mol and ω_e = 958.5 cm^{-1}, are in good agreement with the experimental values,[10] T_0 = 98.26(7) kcal/mol and ω_e = 971(24) cm^{-1}.

We discuss now separately the $17^4\Pi(3)$ (BC) and $19^4\Pi(3)$ (AlC) states. Concerning the BC system, as we move from infinity, B (^{4}P; ±1) + C (^{3}P; 0), its PEC (Figure 8) suffers a first avoided crossing around 4.2 bohr with the lower $15\Pi^4(2)$ state resulting at this point in a local minimum with a depth of 34.6 kcal/mol with respect to the asymptotic products. A second avoided crossing occurs around 4 bohr with the incoming $21^4\Pi(4)$ state which transfers its infinity character B (^{4}P; 0) + C (^{3}P; ±1), to the equilibrium of the $17^4\Pi(3)$ state. The global (G) genuine minimum has a D_e = 53.8 kcal/mol at r_e = 1.599 Å. The bonding is similar to that of the $^4\Pi(1)$ state consisting of $^3/_2\pi$ and $^1/_2\sigma$ bonds, but with the latter originating from the C instead from the B atom.

The $19^4\Pi(3)$ PEC of AlC, (Figure 9) behaves similarly to the $17^4\Pi(3)$ of BC, but there are some differences. It correlates to Al (^{2}S-Rydberg) + C (^{3}P; ±1); this character is conserved up to about 6.5 bohr where it experiences an avoided crossing with the $20^4\Pi(4)$ higher state correlating to Al (^{4}P; ±1) + C (^{3}P; 0). Around 4.7 bohr, as a result of a second avoided crossing with the lower $13^4\Pi(2)$ state, a first local (L) minimum is created with a D_e = 35.5 kcal/mol with respect to Al (^{2}S-Rydberg) + C (^{3}P). A final, third avoided crossing at 4.2 bohr with the $20^4\Pi(4)$ state, transfers the latter's character to the (genuine) global minimum at r_e = 1.982 Å and D_e = 36.6 kcal/mol with respect to Al (^{2}S-Rydberg) + C (^{3}P), or 42.0 kcal/mol with respect to Al (^{4}P) + C (^{3}P) (internal bond strength). The bonding, as before, consists of $^3/_2\pi$ and $^1/_2\sigma$ bonds.

Our last calculated $^4\Pi$ states, $\mathbf{21^4\Pi(4)}$ (BC) and $20^4\Pi(4)$ (AlC), correlate to B (^{4}P; 0) + C (^{3}P; ±1), and Al (^{4}P; ±1) + C (^{3}P; 0), respectively. The corresponding PEC's are shown in Figures 8 and 9.

In the BC system the PEC's infinity character is conserved up to 4 bohr, with about 10% involvement of the B (^{2}P; ±1) + C (^{5}S) between 6.5 and 5 bohr. At 4 bohr the $21^4\Pi(4)$ state experiences and avoided crossing with the lower $17^4\Pi(3)$ state (vide supra), resulting in local (L) minimum at 4.01 bohr (= 2.12 Å). A second avoided crossing with an incoming (not calculated) $^4\Pi(5)$ state correlating most probably to B (^{4}P; ±1) + C (^{1}D; 0), transfers its character to the global (G) genuine minimum at r_e = 1.602 Å and D_e = 32.5 kcal/mol with respect to the asymptotic fragments, or 61.8 kcal/mol (internal bond strength) with respect to B (^{4}P) + C (^{1}D).

As we move now from infinity to the left in the AlC system, Figure 9, the asymptotic character is maintained up to 6.5 bohr. At this point an avoided crossing occurs with the lower $19^4\Pi(3)$ state having the character of Al (^{2}S-Rydberg) + C (^{3}P; ±1), while at 5.2 bohr a second avoided crossing occurs with the (partially) calculated $^4\Pi(5)$ state correlating to Al (^{4}P; 0) + C (^{3}P; ±1). A third avoided crossing at 4.2 bohr with the lower $19^4\Pi(3)$ state, but with the character Al (^{2}P; 0) + C (^{3}P; ±1), gives rise to a global (G) "minimum" at r_e = 4.28 bohr (= 2.27 Å) and D_e = 32.3 kcal/mol with respect to the asymptote. Moving further to the left, a final avoided crossing intervenes around 3.9 bohr with the $^4\Pi(5)$ state which itself had already suffered at least two avoided crossings, leading to a genuine local (L) minimum at r_e = 3.742 bohr = (1.980 Å) and D_e = 26.4 kcal/mol with respect to the adiabatic fragments, or D_e = 55.7 kcal/mol (internal bond strength) with respect to Al (^{4}P; ±1) + C (^{1}D; 0).

$11^4\Delta(1)$, $22^4\Delta(2)/9^4\Delta(1)$, and $24^4\Delta(2)$. The two $^4\Delta(1)$ states, 11 (BC) and 9 (AlC), Figures 6 and 7, correlate to Z (^{2}P; ±1) + C (^{3}P; ±1), Z = B/Al. For both systems shallow minima are observed at r_e (BC/AlC) = 1.856/2.627 Å with D_e (BC/AlC) = 7.8/1.44 kcal/mol. The weak bonding consists of a $^1/_2$ σ bond due to a slight electron transfer from the C $2p_z$ to an empty p_z Z (B/C) orbital. This is also reflected to the rather small and "negative" dipole moments, μ = −0.186/−0.831 D.

The next $^4\Delta$ states, $22^4\Delta(2)$ and $24^4\Delta(2)$ for BC and AlC, respectively, correlate to Z (^{4}P; ±1) + C (^{3}P; ±1) and present similar structural characteristics along their PECs, Figures 6 and 7. At r_e = 2.230 Å the BC system has a local (L) minimum and D_e = 11.3 kcal/mol, while at r_e = 2.408 Å the corresponding AlC minimum is global (G) with D_e = 16.3 kcal/mol. The bonding, for both systems, comprises of one σ bond between a sp_z Z (B/Al) hybrid and the p_z C orbital, or using vbL diagrams

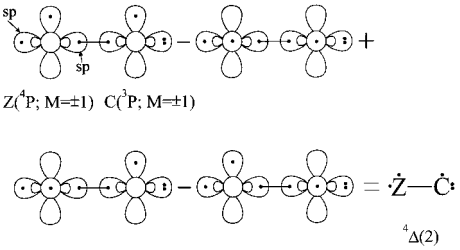

At about 3.5 (BC) and 3.9 (AlC) bohr, avoided crossings take place with the $^4\Pi(3)$ (BC/AlC) state(s) correlating to Z (^{4}P; 0) + C (^{1}D; ±2); this character is transferred to the global (G) BC and local (L) AlC minimum at r_e (BC/AlC) = 1.506/1.893 and D_e (BC/AlC) = 19.2/14.8 kcal/mol. Corresponding D_e values with respect to Z (^{4}P; 0) + C (^{1}D; ±2) are 48.5/45.6 kcal/mol. In both systems the Z (B/Al) and C atoms are held together by a π bond and $^1/_2\sigma$ "interaction".

$20^4\Phi(1)/21^4\Phi(1)$. Due to severe technical difficulties, we were unable to compute potential energy curves of the $^4\Phi(1)$ (BC/AlC) states beyond 3.5/4.2 bohr at the MRCI level of theory, Figures 8 and 9. These states correlate to Z (^{4}P; ±1) + C (^{1}D; ±2), Z = B/Al, and are characterized by r_e (BC/AlC) = 1.583/1.974 Å, and D_e (BC/AlC) = 65.8/60.4 kcal/mol, with bondings consisting of $^3/_2\pi$ and $^1/_2\sigma$ bonds. Overall, less than 0.1 e^- are transferred from B to C, and 0.4 e^- from Al to C, in agreement with the opposite signs of dipole moments, μ (BC/AlC) = −0.15/+0.97 D.

3.2.c. Symmetries $^6\Sigma^+$, $^6\Sigma^-$, $^6\Pi$, *and* $^6\Delta$. $25^6\Sigma^+(1)$, $26^6\Sigma^+(2)/26^6\Sigma^+(1)$, and $28^6\Sigma^+(2)$. All these states, BC/AlC, are purely repulsive (Figures 10 and 11), correlating to fragments listed in Tables 4 and 5. We would like only to report that the $26^6\Sigma^+(2)$ BC potential energy curve shows an avoided crossing around 3.9 bohr, 75 kcal/mol above the asymptote, with a $^6\Sigma^+(3)$ state correlating to B (^{4}P; 0) + C (^{5}S).

$24^6\Sigma^-(1)$, $29^6\Sigma^-(2)/23^6\Sigma^-(1)$, and $30^6\Sigma^-(2)$. The $24^6\Sigma^-(1)$ (BC) and $23^6\Sigma^-(1)$ (AlC) states correlate to Z (^{4}P; ±1) + C (^{3}P; ∓1), Z = B/Al; PECs are shown in Figures 10 and 11. The BC potential energy curve seems to experience a severe avoided crossing at 3.5 bohr, and then presents a minimum at r_e = 2.691 bohr (= 1.424 Å), with a D_e = −4.3 kcal/mol with

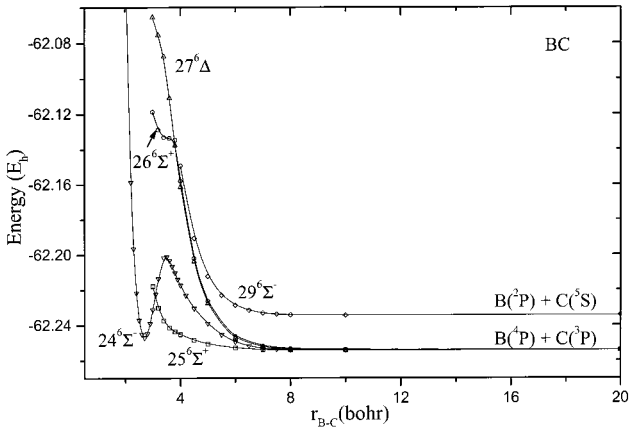

Figure 10. MRCI potential energy curves of sextets $24^6\Sigma^-(1)$, $25^6\Sigma^+(1)$, $26^6\Sigma^+(2)$, $27^6\Delta(1)$, and $29^6\Sigma^-(2)$ of the BC molecule.

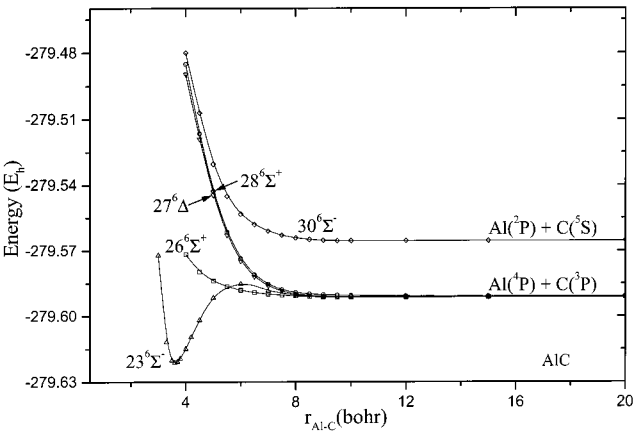

Figure 11. MRCI potential energy curves of sextets $23^6\Sigma^-(1)$, $26^6\Sigma^+(1)$, $27^6\Delta(1)$, $28^6\Sigma^+(2)$, and $30^6\Sigma^-(2)$ of the AlC molecule.

respect to the asymptotic fragments. However, we hasten to express our reservations concerning the PEC's morphology and the fact that this state is unbound with respect to the asymptote, as contrasted to the corresponding AlC state (see below).

In the AlC case, state $23^6\Sigma^-(1)$, the infinity character is transferred to the equilibrium occurring at $r_e = 1.914$ Å, with $D_e = 18.9$ kcal/mol at the MRCI level. The bonding icon shown below suggest the formation of two $^1/_2\,\pi$ bonds.

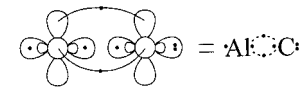

The states $29^6\Sigma^-(2)$ (BC) and $30^6\Sigma^-(2)$ (AlC) correlating to Z (^{2}P; 0) + C(^{5}S), Z = B/Al are purely repulsive, Figures 10 and 11.

$12^6\Pi(1)$, $23^6\Pi(2)$, $28^6\Pi(3)/12^6\Pi(1)$, $25^6\Pi(2)$, and $29^6\Pi(3)$. It is of interest that the first sextet state $12^6\Pi(1)$ of BC and AlC, are strongly bound with respect to their asymptotic fragments Z (^{4}P; ±1) + C (^{3}P; 0), Z = B/Al, Figures 12 and 13. According to the leading CASSCF equilibrium CFs and density distributions, Tables 4 and 5, the bonding is succinctly represented by the following vbL diagram

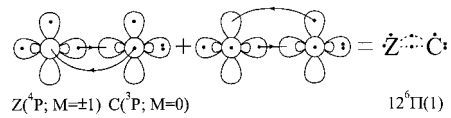

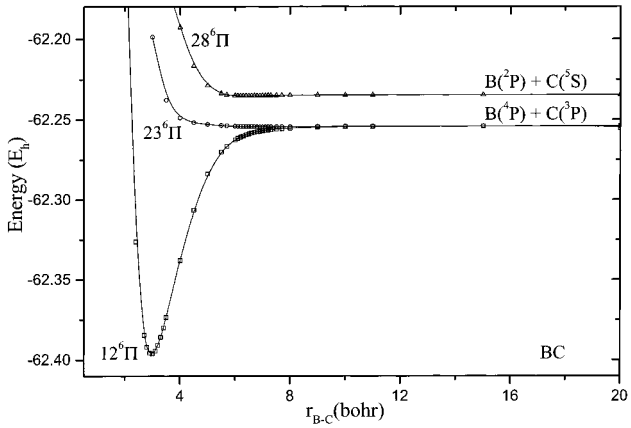

Figure 12. MRCI potential energy curves of sextets $12^6\Pi(1)$, $23^6\Pi(2)$, and $28^6\Pi(3)$ of the BC molecule.

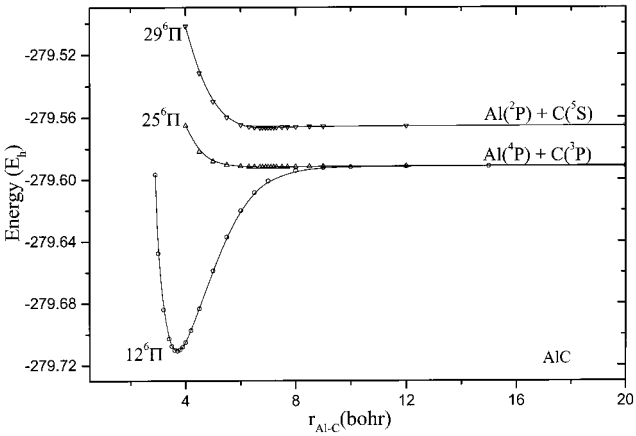

Figure 13. MRCI potential energy curves of sextets $12^6\Pi(1)$, $25^6\Pi(2)$, and $29^6\Pi(3)$ of the AlC molecule.

indicating a $^1/_2\pi$ and $^1/_2\sigma$ bonds. Along the σ frame 0.3/0.5 e^- are transferred from B/Al to the C atom; via the π frame 0.2/0.1 e^- are moving from C to B/Al atoms. Notice also the opposite dipole moments signs between the two systems. At r_e (BC/AlC) = 1.571/1.953 Å a D_e (BC/AlC) = 88.4/74.9 kcal/mol is obtained at the MRCI level, with respect to the asymptotic products, or 5.5/−4.5 with respect to the ground-state atoms.

The rest of the four Π BC/AlC sextets, 23, 28/25, and 29, are practically repulsive, Figures 12 and 13. Their "binding" energies range from 0.24 ($23^6\Pi(2)$) to 0.61 ($29^6\Pi(3)$) kcal/mol.

$27^6\Delta(1)/27^6\Delta(1)$. Both these states correlating to Z (^{4}P; ±1) + C (^{3}P; ±1), Z = B/Al, are purely repulsive, Figures 10 and 11. In the case of the BC system an avoided crossing takes place at 2.5 bohr.

4. Synopsis and Remarks

In the present report we have examined in some detail 29 and 30 excited states of the BC and AlC systems, using multireference methods coupled with large correlation consistent basis sets. Results of the ground $X^4\Sigma^-$ (BC/AlC) states have been reported elsewhere.[1] For both molecules and for all 29 and 30 states we have constructed complete potential energy curves at the multireference−CISD level, and we have calculated dissociation energies, bond lengths, dipole moments, and the most common of spectroscopic constants. Judging from our previous work on these systems,[1] and the very good agreement with existing, although limited experimental results, we are confident of the quantitative nature of our findings.

Our most general results are the following.

(1) There is a close correspondence among the spectroscopic states of the BC and AlC molecules. For instance, both are characterized by a $^4\Sigma^-$ ground and $^2\Pi$ first excite state, with bonding of similar nature. The way that states of the same symmetry are related is shown in Figure 1.

(2) The binding energies range from 102 ($X^4\Sigma^-$) to about 1 kcal/mol in the BC system; the corresponding values in AlC are 80 to 1 kcal/mol with respect to the asymptotic products. With respect to the diabatic products, the largest internal bond strengths are 159.0 ($4^4\Pi(1)$) and 107.2 kcal/mol ($6^4\Pi(1)$) for the BC and AlC, respectively.

(3) The bonding of both molecules is depicted by valence bond−Lewis icons based on the dominant configurations of the reference space and the Mulliken population analysis. The bonding characters range from a half bond to two π bonds and a σ interaction.

(4) The r_e values varies from 1.322 ($9^2\Sigma^+(2)$) to 2.077 Å ($18^4\Sigma^-(2)$) and from 1.753 ($14^2\Sigma^+(2)$) to 3.759 Å ($10^2\Sigma^-(2)$) for the BC and AlC molecules, respectively.

(5) Out of the 29/30 excited states studied, 15 states for the BC and 11 for the AlC systems are bound with respect to ground-state atoms.

(6) Several states show avoided crossings while six/five of the states present two minima, a local (L) and a global (G), i.e., $10^2\Delta(2)$, $14^2\Sigma^-(2)$, $16^2\Pi(4)$, $17^4\Pi(3)$, $21^4\Pi(4)$ and $22^4\Pi(2)$/$15^2\Pi(2)$, $18^4\Sigma^-(3)$, $19^4\Pi(3)$, $20^4\Pi(4)$, and $24^4\Pi(2)$, BC/AlC.

(7) In the BC molecule, −0.1 to 0.2 e^- are transferred from B to C, and in the AlC molecule up to 0.5 e^- are transferred from Al to C.

(8) The dipole moments vary from 3.13 ($16^2\Pi(4)$) to −1.58 D ($10^2\Delta(2)$) for the BC molecule and 8.84 ($18^4\Sigma^-_L(3)$) or 3.22 ($14^2\Sigma^+(2)$) to −0.831 D ($9^4\Delta(1)$).

(9) The harmonic frequencies (ω_e) range from a minimum value of 41.2 ($23^6\Pi(2)$)/43.8 ($25^6\Pi(2)$) to a maximum of 1722.3 ($9^2\Sigma^+(2)$)/1023.6 cm^{-1} ($20^4\Pi(4)$) for the BC/AlC molecule, thus reducing the corresponding D_e's by 0.06/0.06 to 2.46/1.46 kcal/mol.

(10) The T_e's of the following pairs or groups differ less than 1 mhartree, and the ordering is possible to be different ($2^2\Sigma^-$, $3^2\Delta$, $4^4\Pi$), ($11^4\Delta$, $12^6\Pi$) and ($13^4\Sigma^+$, $14^2\Sigma^-$)/($10^2\Sigma^-$, $11^4\Sigma^+$) and ($14^2\Sigma^+$, $15^2\Delta$) for the BC/AlC molecules. The ordering is reversed by adding the zero point energy correction $\Delta\omega_e/2$ only for the pair ($14^2\Sigma^+$, $15^2\Delta$) of the AlC molecule by 0.2 kcal/mol. Last, by applying the Davidson +Q correction, the ordering is reversed for the groups ($12^6\Pi$, $13^4\Sigma^+$, $14^2\Sigma^-$)/($2^2\Sigma^-$, $3^2\Delta$), ($12^6\Pi$, $13^4\Pi$), ($14^2\Sigma^+$, $15^2\Delta$), and ($23^6\Sigma^-$, $24^4\Delta$) for the BC/AlC molecules.

Acknowledgment. D.T. expresses her gratitude to the Hellenic Scholarship Foundation (IKY) for financial assistance.

References and Notes

(1) Tzeli, D.; Mavridis, A. *J. Phys. Chem. A* **2001**, *105*, 1175.
(2) Verhaegen, G.; Stafford, F. E.; Drowart, J. *J. Chem. Phys.* **1964**, *40*, 1622.
(3) Fernando, W. T. M. L.; O'Brien, L. C.; Bernath, P. F. *J. Chem. Phys.* **1990**, *93*, 8482.
(4) Thoma, A.; Caspary, N.; Wurfel, B. E.; Bondybey, V. E. *J. Chem. Phys.* **1993**, *98*, 8458.
(5) Brazier, C. R. *J. Chem. Phys.* **1993**, *98*, 2790.
(6) Kouba, J. E.; Öhrn, Y. *J. Chem. Phys.* **1970**, *53*, 3923.
(7) Zaitsevskii, A. V.; Dement'ev, A. I.; Zviadadze, G. N. *J. Less-Common Met.* **1986**, *117*, 237.
(8) Hirsch, G.; Buenker, R. J. *J. Chem. Phys.* **1987**, *87*, 6004.
(9) Smith, A. M.; Lorenz, M.; Agreiter, J.; Bondybey, V. E. *Mol. Phys.* **1996**, *88*, 247.
(10) Wyss, M.; Grutter, M.; Maier, J. P. *J. Phys. Chem. A* **1998**, *102*, 9106.
(11) Gutsev, G. L.; Jena, P.; Bartlett, R. J. *J. Chem. Phys.* **1999**, *110*, 2928.
(12) Bauschlicher, C. W., Jr.; Langhoff, S. R.; Pettersson, L. G. M. *J. Chem. Phys.* **1988**, *89*, 5747.
(13) Dunning, T. H., Jr. *J. Chem. Phys.*, **1989**, *90*, 1007. Kendall, R. A.; Dunning, T. H., Jr.; Harrison, R. J. *J. Chem. Phys.* **1992**, *96*, 6796.
(14) Werner, H.−J.; Knowles, P. J. *J. Chem. Phys.* **1988**, *89*, 5803. Knowles, P. J.; Werner, H.−J. *Chem. Phys. Lett.* **1988**, *145*, 514. Werner, H.-J. Reinsch, E. A. *J. Chem. Phys*. **1982**, *76*, 3144. Werner, H.-J. *Adv. Chem. Phys.* **1987**, *LXIX*, 1.
(15) Tzeli, D.; Mavridis, A. *J. Phys. Chem. A* **2000**, *104*, 6861. Kalemos, A.; Mavridis, A. *J. Phys. Chem. A* **1998**, *102*, 5982.
(16) Docken, K.; Hinze, J. *J. Chem. Phys*. **1972**, *57*, 4928. Werner, H.−J.; Meyer, W. *J. Chem. Phys.* **1981**, *74*, 5794.
(17) Moore, C. E. Atomic Energy Levels. NSRDS−NBS Cirular No. 35; National Bureau of Standards: Washington, DC, 1971.
(18) MOLPRO 96 is a package of ab initio programs written by Werner, H.−J.; Knowles, P. J. with contributions by Almlof, J.; Amos, R. D.; Berning, A.; Deegan, M. J. O.; Eckert, F.; Elbert, S. T.; Hampel, C.; Lindh, R.; Meyer, W.; Nicklass, A.; Peterson, K.; Pitzer, R.; Stone, A. J.; Taylor, P. R.; Mura, M. E.; Pulay, P.; Schuetz, M.; Stoll, H.; Thorsteinsson, T.; Cooper, D. L.
(19) Langhoff, S. R.; Davidson, E. R. *Int. J. Quantum Chem.* **1974**, *8*, 61. Blomberg, M. R. A.; Sieghbahm, P. E. M. *J. Chem. Phys.* **1983**, *78*, 5682.
(20) See for instance: Gaydon, A. G. *Dissociation Energies and Spectra of Diatomic Molecules*; Chapman and Hall.: London, 1968.